MICROBIOTA-DERIVED D-LACTATE ALTERS MACROPHAGE INFLAMMATION

MICROBIOTA-DERIVED D-LACTATE ALTERS NITRIC OXIDE AND INFLAMMASOME IMMUNITY IN MACROPHAGES

by Anita Marie Singh, BHSc.

A Thesis Submitted to the School of Graduate Studies in Partial Fulfilment of the Requirements for the Degree of Master of Science

McMaster University MASTER OF SCIENCE (2022) Hamilton, Ontario

(Biochemistry)

TITLE: Microbiota-derived D-lactate alters macrophage inflammation

AUTHOR: Anita Marie Singh, BHSc (McMaster University)

SUPERVISOR: Dr. Jonathan D. Schertzer

NUMBER OF PAGES: xiii, 83

Lay Abstract

Gut bacteria can influence both immunity and metabolism in the liver. It is not clear how bacteria in the gut communicate to the liver. Lactate is a key metabolite that can fuel liver metabolism and alter immunity. There are 2 types of lactate. L-lactate is host-derived, whereas D-lactate is mainly produced by gut bacteria. Bacterial-derived D-lactate can alter immune responses mediated by immune cells in the liver, including macrophages. Bacterial metabolites such as D-lactate and bacterial components that cause inflammation are increased in the blood during obesity. Our findings show that D-lactate can increase inflammation in macrophages when combined with bacterial components and that D-lactate increases inflammation more than L-lactate. Understanding the role of D-lactate may help us understand how bacteria contribute to insulin resistance, higher blood glucose and the risk of type 2 diabetes and fatty liver disease.

Abstract

Obesity-induced inflammation is a factor involved in the risk and progression of type 2 diabetes and non-alcoholic fatty liver disease. These diseases are associated with changes in gut microbiota composition and bacterial metabolites. Bacterial components with known innate immune receptors can cooperate with non-immunogenic metabolites derived from the gut microbiota to alter host immunity. Gut bacteria produce almost all D-lactate in the host, whereas L-lactate is host-derived. It is known that microbial-derived D-lactate in the portal circulation programs liver-resident macrophages to help combat bacterial infections. It was unknown how D-lactate and L-lactate alter cell-autonomous inflammation in macrophages exposed to low levels of bacterial cell wall muropeptides or lipopolysaccharide (LPS). It was also unknown if macrophage co-stimulation altered inflammation in macrophages exposed to bacterial metabolites and cell wall components. *In vitro* models showed that D-lactate had no effect (or a very small effect) on multiple markers of inflammation in the absence of interferon-gamma (IFN-γ) co-stimulation. Nevertheless, initial experiments on clonal macrophages discovered that equimolar and physiological levels of D-lactate increased *Nos2* expression compared to L-lactate. Bone marrow-derived macrophages (BMDMs) co-stimulated with IFN-γ revealed a larger effect of D-lactate on immunity. Compared to L-lactate, D-lactate increased nitric oxide (NO) production and increased activation of the NLR family pyrin domain containing 3 (NLRP3) inflammasome in BMDMs co-stimulated with IFN-γ

and exposed to LPS. Further, D-lactate prevented L-lactate-induced lowering of NO production and NLRP3 inflammasome-mediated release of IL-1β from BMDMs co-stimulated with IFN-γ and LPS. Identifying appropriate cell models and defining conditions that reveal the effect of D-lactate versus L-lactate on immune responses in isolated cells was a major contribution of this work. Future work should characterize the interaction of macrophages and hepatocytes. This research may lead to the identification of gut microbiota-based approaches to limit liver inflammation in obesity and metabolic disease.

ACKNOWLEDGEMENTS

I would like to acknowledge the many individuals who have helped and contributed to this project, without whom the successful completion of my thesis would not be possible. First, I would like to give my most sincere thanks to Dr. Jonathan Schertzer. Thank you for helping me to navigate graduate school and the pressures of research during a global pandemic. Your continual support, guidance and encouragement has not gone unnoticed, for which I am very grateful. Your mentorship has truly had a positive impact on me, and it has been an absolute pleasure to learn from you.

I would like to extend a special thank you to Dr. Brittany Duggan for sharing your knowledge of lab techniques and to Dr. Fernando Forato Anhê for your wisdom and guidance. Thank you to Dr. Nicole Barra for your continual support and for helping me with experiments and analyses. I would also like to acknowledge my colleagues: Dr. Hannah Fang, Dr. Rodrigo Lacerda, Darryl Chan, Arshpreet Bhatwa, Danny Marko, and Nazli Robin. Thank you for making every day a great experience. I wish you all the very best in your future endeavours.

Thank you to my supervisory committee Dr. Dawn Bowdish and Dr. Gregory Steinberg for your guidance, advice, and willingness to help me succeed.

Finally, I would like to thank all my friends and family for their support and encouragement throughout my graduate studies.

TABLE OF CONTENTS

LIST OF FIGURES

LIST OF TABLES

LIST OF ABBREVIATIONS

3-OBA	3-hydroxy-butyrate acid
ANOVA	Analysis of variance
ATP	Adenosine triphosphate
BMDM	Bone marrow-derived macrophage
cDNA	Complementary deoxyribonucleic acid
DMEM	Dulbecco's modified eagle medium
DMEM/F-12	Dulbecco's modified eagle medium/nutrient mixture F-12
ELISA	Enzyme-linked immunosorbent assay
FBS	Fetal bovine serum
GPR81	G-coupled protein receptor 81
GF	Germ-free
GM-CSF	Granulocyte-macrophage colony-stimulating factor
HEK	Human embryonic kidney
IFN-γ	Interferon-gamma
IL-18	Interleukin-18
IL-1β	Interleukin-1beta
IL-12	Interleukin-12
IL-6	Interleukin-6
iNOS	Inducible nitric oxide synthase
LPS	Lipopolysaccharide
M-CSF	Macrophage colony-stimulating factor
MCT	Monocarboxylate transporter
NF-κB	Nuclear factor-kappa B

NLRP3	NOD-, LRR- and pyrin domain-containing protein 3
NO	Nitric oxide
NOD1	Nucleotide-binding oligomerization domain-1
P/S	Penicillin/streptomycin
PAMP	Pathogen associated molecular pattern
PBS	Phosphate buffered saline
RNA	Ribonucleic acid
ROS	Reactive oxygen species
RT-PCR	Real-time polymerase chain reaction
SCFA	Short-chain fatty acid
SEM	Standard error of the mean
T2D	Type 2 diabetes
TLR	Toll-like receptor
TNF	Tumour necrosis factor
Treg	Regulatory T cell
αCHC	α-Cyano-4-hydroxycinnamic acid

DECLARATION OF ACADEMIC ACHIEVEMENT

The following is a declaration that the content of the research presented in this thesis has been completed by Anita Marie Singh, with some assistance from Dr. Fernando Forato Anhê with animal studies. The research study was designed by Dr. Jonathan Schertzer, who also contributed to the review and completion of this thesis. To the best of my knowledge, the content of this thesis does not infringe on the copyright of any others.

1.0 INTRODUCTION

1.1 Obesity and type 2 diabetes

Obesity is a chronic and progressive disease that is characterized by excessive adipose tissue expansion and dysglycemia. The obesity epidemic has seen a dramatic increase in prevalence among children and adults over the last three decades[1]. Obesity has a significant cost to society and its economic burden includes increased health care expenditures[2,3]. The causes of obesity are multifactorial and complex and include genetic, environmental, socioeconomic, and behavioural factors. Obesity increases the risk of several other chronic diseases including heart disease, type 2 diabetes (T2D), non-alcoholic fatty liver disease (NAFLD), stroke, and cancer among others[1,4,5]. It is estimated that by 2025, over 300 million individuals worldwide will have developed T2D from obesity[6].

Lowering caloric intake has been shown to reduce obesity, but long-term adherence to these diets is a major concern[7,8]. Bariatric surgery lowers intestinal nutrient absorption and is currently the most efficacious treatment for obesity and T2D, but is limited in accessibility and feasibility at the population level that would be required to combat T2D and NAFLD [9,10]. Further, potential surgical candidates must show previous attempts at improving obesity using medical interventions and must be committed to changing their behaviour and nutritional intake long-term[9]. The economic, societal, and direct and indirect medical ramifications of the growing obesity epidemic are severe. Therefore, there is an urgent need to

discover non-surgical modifiers of intestinal nutrient absorption to mitigate the risk of developing co-morbidities.

1.1.1 Obesity-induced inflammation and co-morbidities

Obesity promotes compartmentalized inflammation that contributes to mechanisms of T2D and NAFLD progression, including insulin resistance and pancreatic β-cell dysfunction. Excessive adipose tissue expansion due to an imbalance between nutrient intake and energy expenditure is a major feature of obesity[11,12]. Adipose tissue expansion is associated with chronic low-grade inflammation in adipose tissue and the liver, called metabolic inflammation[12]. There are many triggers of this metabolic inflammation during obesity which include changes in adipokines, lipid homeostasis and the gut microbiota that affect metabolic cells like adipocytes, and immune cell populations in metabolic tissues[13–15]. Obesity-induced inflammation also promotes NAFLD progression to non-alcoholic steatohepatitis (NASH) where inflammation affects hepatocytes and resident immune cells[16,17]. There is an urgent need to identify contributors to obesity-induced inflammation and mitigate the risk of T2D and NAFLD. It is intriguing that targeting metabolites akin to modifiers of intestinal nutrient absorption from the gut microbiota might alter obesity-related inflammation.

Nutritional stress sensed by immune receptors contributes to obesity-induced inflammation[18]. Pattern recognition receptors (PRRs) such as toll-like receptors (TLR) and nucleotide oligomerization domain (NOD)-like receptors play a crucial role in innate immunity by responding to pathogen-associated molecular

patterns (PAMPs) and damage-associated molecular patterns (DAMPs)[18,19]. Microbial components like lipopolysaccharide (LPS) can activate TLR signalling via a MyD88-dependent pathway leading to the activation of nuclear factor kappa B (NF-κB) thereby amplifying cytokine production[18,20]. TLR2 and TLR4 have been shown to play a role in promoting obesity-induced inflammation and subsequent insulin resistance[21]. TLR4 is localized to the surface of immune cells like macrophages and metabolic cells like hepatocytes and adipocytes and is increased in obese mice and humans with obesity. Diet-induced changes in gut microbiota composition and gut permeability during obesity contribute to metabolic endotoxemia (an increase in circulating LPS) which engages TLR4 to promote features of prediabetes and NAFLD progression[22–25].

1.2 Gut microbiota

The microbiota that reside on (and in) humans is thought to contain over 30 trillion bacteria, fungi and viruses. Most bacteria reside in the gut and the gut microbiota describes all microbial strains that reside within the gastrointestinal tract. The role of the gut microbiota in metabolic disease has recently emerged as a popular area of research. The gut microbiota play a key role in supporting the digestion of nutrients that are not metabolized by human enzymes. It is known that commensal bacteria in the gut influence host metabolism, digestion, brain and immune function[26].

The composition of the microbiota varies between individuals and is influenced by medication, diet, genetics, and a variety of environmental factors[26]. Changes in taxonomy and relative abundance of bacterial species can serve as a biomarker for disease onset or progression. For example, *Lactobacillus reuteri* and *Lactobacillus intestinalis* have been associated with human obesity and obesity-induced T2D[27,28]*.* Bacterial components, metabolites and secreted microbial factors can engage host immunity to influence host metabolism and can influence aspects of health and disease by communicating with peripheral organs through various pathways (i.e., gut-liver axis)[26]. Microbial-derived factors from the gut can communicate with the liver via portal circulation[29,30]. Many specific bacterial components and metabolites that cooperate to alter immunity or metabolism remain ill-defined.

1.2.1 Gut microbiota and metabolic disease

Microbiota participate in host obesity and T2D progression through many different proposed mechanisms, which is often attempted to be captured by measuring changes in gut microbiome taxonomy or metabolites[31]. Studies of colonization of germ-free (GF) mice by transplantation of gut microbiota from conventionalized obese mice and obese humans have demonstrated that gut microbes are sufficient to transfer obesity phenotypes such as increased adiposity from obese microbial donors to lean recipients[32–34]. Further, there are marked differences in microbial populations at the taxonomic level between humans that are obese or not obese. Peters *et al*. recently found that species

richness and overall composition were reduced in obese, but not overweight individuals, compared to humans classified as normal weight[35]. This study found an increase in the abundance of Streptococcaceae and Lactobacillaceae, and a decreased abundance of within classes Clostridia, Christensenellaceae, Clostridiaceae, and Dehalobacteriaceae[35]. Changes in abundance and richness of microbial species correlated with obesity may offer insight into species-specific metabolites that exacerbate inflammation and insulin resistance.

Evidence suggests that changes in the relative abundance of gut commensal bacteria also correlate with changes in glucose homeostasis[30,36]. It is known that the composition of the gut microbiome is altered in obese mice and humans with impaired glucose metabolism[37,38]. We have previously shown that gut microbiota regulate insulin clearance in diet-induced obese mice[39]. Antibiotic treatment of obese mice, including hyperphagic *ob/ob* mice and diet-induced obese mice, improved glucose tolerance and lowered insulin resistance, which was thought to occur by reducing the load of bacteria and/or by altering some features of dysbiosis in the gut commensal population[40]. Lowering the intestinal microbe load with antibiotics also reduced the expression of hepatic and intestinal genes associated with inflammation and lipid metabolism[40]. Further, GF mice have lower liver fat, lower lipogenic gene signature, and reduced inflammation in adipose tissue compared to colonized mice, which contributes to impaired glucose metabolism[26,33]. Recent evidence showed that gut microbiota can regulate blood glucose homeostasis solely via hepatic gluconeogenesis and

not via energy expenditure, but the bacterial metabolite that acted as a substrate to drive changes in liver metabolism was unknown[41,42]. Hence, there is data showing that gut commensal bacteria play a key role in altering liver metabolism and inflammation relevant to the pathophysiology of T2D and NAFLD. We sought to find a microbial factor that could influence liver metabolism and inflammation.

1.2.2 Microbial-derived metabolites and host immunity

The interaction between gut microbiota and peripheral organs beyond the intestine, such as the liver, may involve innate immunity including TLR and/or NOD-like receptor signalling in response to translocation of microbial components across the intestinal barrier and into host circulation. TLRs are a class of PRRs that are expressed on the cell surface or endosomes of innate and non-innate immune cells[20]. These receptors are responsible for recognizing lipids, proteins or nucleic acids that can be specific to PAMPs like bacteria[20]. Specifically, TLR4 recognizes lipid A of bacterial lipopolysaccharides (LPS)[20]. Recognition of a PAMP by a TLR initiates a signalling pathway leading to downstream activation of NF-κB which regulates the expression of cytokines and chemokines to elicit an innate immune response against the microbial danger signal[20]. The microbiota composition can influence TLR activation and lower insulin sensitivity[43]. NOD-like receptor signalling may also be implicated in microbe-immune interactions occurring in tissues that help control blood glucose such as the liver. NOD1 is expressed in the cytosol of hepatocytes and responds to FK565 and γ-d-glutamyl-meso-diaminopimelic acid (iE-DAP) found in the cell

wall structure of most Gram-negative bacteria[19]. NOD1 ligands, but not NOD2 ligands, were shown to activate NF-κB in primary mouse hepatocytes *in vitro*[44]. IFN-γ is a co-stimulatory factor produced by T cells that promotes M1 polarization in macrophages[45]. Also, we have previously shown that NOD1 ligand co-stimulation with IFN-γ was required to measure changes in inflammation in primary hepatocytes[46].

Interactions between microbial-derived metabolites and cell wall components are positioned to alter the activation of resident immune cells in hepatic and adipose tissues but how these microbial-derived metabolites (such as D-lactate) can modulate the effect of TLR4 and NOD1 ligands on hepatic or adipose tissue inflammation is unknown.

1.3 The Cori cycle

The Cori cycle describes the mechanism by which glycogen is metabolized in skeletal muscle via anaerobic glycolysis to produce lactate, which in turn provides a substrate for liver glycogen storage and gluconeogenesis (Figure 1)[47]. Muscle glycogen breakdown is facilitated by lactate dehydrogenase (LDH), an oxidoreductase that reversibly catalyzes the conversion of pyruvate to lactate with the regeneration of NADH. LDH plays a key role in maintaining homeostasis under anaerobic conditions. Since oxygen is the final electron acceptor in the electron transport chain, when oxygen availability is low, adenosine triphosphate (ATP) synthesis via ATP synthase is limited. Despite ATP production via oxidative phosphorylation being disrupted in anaerobic

conditions, ATP synthesis continues in the muscle from the reduction of pyruvate to lactate and generation of NAD+[48]. L-isomers of LDH produce L-lactate, which is the most abundant lactate isomer in vertebrates[48]. Lactate can then travel through the blood and be used as a substrate for hepatic gluconeogenesis. Thus, L-lactate is a key substrate fueling glucose synthesis under anaerobic conditions.

1.3.1 Lactate enantiomers: D-lactate and L-lactate

D-lactate metabolism has been historically overlooked. When the Cori cycle was first described, D-lactate extracted from bacteria was used, as it was observed that L-lactate formed “practically no liver glycogen”[47]. However, humans and rodents have ~1000 times higher levels of L-lactate (mM) than D-lactate (µM) in the systemic circulation, which appears to have set the stage for neglecting the study of D-lactate. In the past, it was also hypothesized that mammals lacked D-α-hydroxy acid dehydrogenase, which was thought to be required for D-lactate metabolism[49]. However, we now know that mammals have both L- and D-lactate dehydrogenases[50,51]. Despite its key role in the discovery of the Cori cycle in 1929, the role of D-lactate has not been well investigated in metabolic disease.

D-lactate and L-lactate enantiomers share similar chemical and physical properties. Monocarboxylate transporters (MCT1-8) can transport both L- and D-lactate[49]. MCT1 transports D-lactate in the small intestine and liver; however, MCT1 has a two-times greater uptake coefficient for L-lactate than D-lactate[49]. Transport capacity is not the only factor to consider since local sources of D-

versus L-lactate may influence tissue uptake and metabolism. It was hypothesized that microbial-derived D-lactate may be preferentially shuttled by MCT1 to the liver via the portal circulation, whereas L-lactate is excreted in urine or shuttled by G-coupled protein receptor 81 (GPR81) in the brain, muscle and adipose tissue[52]. L-lactate and D-lactate are derived from different sources, but both can be used as fuel by the liver to produce glycogen. L-lactate is host-derived via anaerobic glycolysis in skeletal muscle. It is thought that glyoxalase 1 and 2 are key enzymes that catalyze the conversion of methylglyoxal into D-lactate, providing low levels of host-derived D-lactate into the circulation[53]. We have previously shown that most D-lactate in mice is derived from gut microbiota, whereas L-lactate is host-derived in fasted and fed mice (unpublished, 2020). Certain bacteria can produce more D-lactate, which can enter host circulation. For example, colonization of mice with the gut microbe *Lactobacillus intestinalis* ASF360 has been shown to produce higher levels of D-lactate in the portal and systemic circulation[29].

In the systemic circulation of mice, we measured physiological levels of L-lactate (1-10 mM) and D-lactate (25-100 µM). Levels of L-lactate and D-lactate are dynamic and can be influenced by the diet, varying levels of exercise, and ageing[49,54,55]. We defined physiological levels of L-lactate and D-lactate as being measured in the systemic circulation of fasted, chow-fed male C57BL/6 N mice during normal levels of exercise and the absence of pathology.

Certain pathological conditions favour elevated levels of D-lactate and/or L-lactate. For example, levels of D-lactate are elevated due to increased production by gut microbiota and impaired gut permeability in patients with ulcerative colitis, short bowel syndrome, and gut ischemia[56,57]. D-lactate and L-lactate are elevated in urine and plasma of T2D patients[58,59]. Further, elevated D-lactate in obese adolescents is associated with higher levels of small dense low-density lipoprotein[60]. It has also been suggested that highly fermented foods may increase circulating levels of L-lactate or D-lactate[49]. Elevated levels of L-lactate in the brain are correlated with ageing, however, the role of D-lactate is not clear[55,61].

1.4 The role of lactate in host immunity

Bacteria in the gut can simultaneously provide PAMPs and metabolites that might co-operate to alter immune responses. Classical examples of immunomodulatory metabolites are short-chain fatty acids (SCFA). Clostridia species are high producers of SCFAs which have been shown to induce regulatory T (Treg) cells and inhibit NF-κB[62]. Certain bacterial-derived metabolites such as SCFAs do not have known immune receptors that could serve as a direct link to immune signalling. However, SCFAs have emerged as important modulators of inflammatory responses by co-operating with immunogenic microbial components[62,63]. Similarly, lactate is a non-immunogenic metabolite and there is no known immune receptor, however, it may engage other microbial components to modulate immune responses like SCFA.

Microbial-derived D-lactate, and specifically its role in inflammation, has rarely been referenced in the literature. This is a key knowledge gap since D-lactate levels are increased in plasma and urine in patients with diabetes and obesity[58,60,64].

The inhibition and downregulation of lactate dehydrogenase A (LDHA), the enzyme that catalyzes the conversion of pyruvate to lactate, suppresses inflammation in RAW 264.7 macrophage-like cells[65]. Inhibition and downregulation of LDHA using siRNA in RAW 264.7 macrophages resulted in lower LPS-stimulated lactate levels and lower interleukin-6 (IL-6), nitric oxide (NO) and inflammatory cytokine production[65]. Although it is unclear from this study whether L-lactate, D-lactate or racemic lactate (a mixture of equal parts D-/L-lactate) was measured, this evidence supports the role of lactate in modulating immunity in macrophages.

The effect of lactate on inflammatory responses relating to tumour microenvironments has been investigated. Importantly, tumours prefer to undergo anaerobic glycolysis leading to high levels of lactic acid in tumour microenvironments[66]. Tumour-derived lactic acid accumulation contributes to pro-tumour, anti-inflammatory microenvironments that promote tumour growth. The levels of lactic acid in the tumour microenvironment can promote M2 phenotypes in tumour-associated macrophages, inhibit dendritic cell function, and decrease cytotoxic T-cell proliferation and function[66–68]. These studies used sodium lactate or lactic acid (10-25 mM) (where the enantiomer was unspecified), but the role of

D-lactate is not clear. Most available evidence suggests that lactate has anti-inflammatory effects in tumour microenvironments to promote tumour growth.

In response to bacterial infection and other sources of inflammation, L-lactate or racemic lactate generally suppress pro-inflammatory responses. L-lactate (15 mM) suppressed TLR4-mediated priming of the NLRP3 inflammasome via suppressed caspase-1 cleavage, mature caspase-1 activity and IL-1β release in bone marrow-derived macrophages, which required GPR81[69]. Similarly, it was shown that racemic lactate inhibits the pro-inflammatory programming of macrophages, although independent of GPR81[70]. In this study, bone marrow-derived macrophages (BMDMs) treated with LPS and varying concentrations of racemic lactate (1-100 mM) dose-dependently inhibited LPS-induced pro-inflammatory markers[70]. Further, in the context of chronic inflammation, extracellular lactate (10 mM sodium L-lactate) inhibits the effector functions of CD4+ T cells and upregulates the lactate transporter SLC5A12[71]. Importantly, lactate-induced inhibition of CD4+ T cell effector function (i.e., motility) was due to changes in glucose metabolism in response to lactate uptake, which involved reduced glycolysis and a shift towards the TCA cycle that promoted fatty acid synthesis[71]. This is a prime example of indirect lactate-induced inhibition of an inflammatory response by altering glucose metabolism and favouring *de novo* fatty acid synthesis. Although there is some evidence regarding the role of lactate in inflammation, little is known about the effect of L- vs D-lactate on inflammation.

There is conflicting evidence to suggest that lactate modulates the pro-inflammatory and anti-inflammatory responses of immune cells upon LPS activation. Few studies have shown that D-lactate has pro-inflammatory influences on immunity. In bovine synoviocytes, D-lactate, but not L-lactate, induces an MCT1-dependent increase in IL-6 and IL-8 expression[72]. Additionally, a recent seminal paper showed that microbiota-derived D-lactate programs tissue-resident macrophages of the liver to clear circulating pathogens during bacterial sepsis[29]. The portal vein directly connects the gut and liver which facilitates communication from gut commensals through metabolites and other soluble mediators. Another key knowledge gap is the effect of physiological doses of L- versus D-lactate on inflammation. Many previous studies use a dose higher than physiological L-lactate (1-10 mM) and do not compare or even test physiological D-lactate (25-100 μM).

Inflammation can alter lipid metabolism and influence the way immune cells respond to inflammatory signals. For example, TLR4 activation in macrophages leads to transient inhibition of fatty acid synthesis followed by a later increase in anti-inflammatory fatty acid synthesis that contributes to the resolution phase of the inflammatory response[73,74]. In a recent study, pro-inflammatory TLR activation in macrophages upregulated lipogenesis via liver X receptor activity[73]. The role of liver X receptors in inflammation and lipogenesis was found to be bidirectional where liver X receptors are also required for suppressing inflammation in the resolution phase[73]. Changes in lipid metabolism

that lead to inflammation are implicated in the progression from NAFLD to NASH[75]. Hepatic steatosis is driven by increased *de novo* lipogenesis which, as previously mentioned, can promote liver inflammation. Rather than being a consequence of steatosis, liver inflammation may also promote a stress response in hepatocytes that leads to lipid accumulation[76]. This was demonstrated when *ob/ob* mice were treated with anti-tumour necrosis factor (TNF) antibodies, inhibiting hepatic TNFα and lowering inflammation and hepatic steatosis[77]. Loss of Kupffer cells has been implicated in hepatic steatosis, and other myeloid cells may be involved in promoting hepatic lipid accumulation via inflammation[78,79].

As discussed, L-lactate was shown to indirectly modulate inflammation by altering glucose metabolism and favouring *de novo* fatty acid synthesis in CD4+ T cells[71]. We propose that inflammation may precede and change the early stages of NAFLD and that a microbial factor such as D-lactate may synergize with bacterial cell wall components to change lipid metabolism and/or inflammation which may exacerbate the progression of NAFLD to NASH (Figure 2).

2.0 RATIONALE, HYPOTHESES AND RESEARCH AIMS

2.1 Rationale

We previously showed that trapping D-lactate, but not L-lactate, in the gut lumen reduces blood D-lactate levels and lowers blood glucose, insulin secretion and insulin resistance in diet-induced obese mice (unpublished, 2020). This data, along with the seminal observation made by McDonald *et al*. that gut microbiota-derived D-lactate programs liver macrophages[29], positions D-lactate as a microbial metabolite that could promote metabolic inflammation in metabolic tissues. D-lactate can promote activation and polarization of macrophages towards pro-inflammatory responses[6,30,45]. We propose that D-lactate is more inflammatory than L-lactate, which we sought to test in macrophages cultured under specific conditions. Thus, microbiota-derived D-lactate is positioned to increase inflammation in resident immune cells of the liver and adipose tissue, contributing to insulin resistance and NAFLD progression.

2.2 Hypothesis

We hypothesize that microbial-derived D-lactate increases macrophage inflammation compared to physiological and equimolar doses of L-lactate in the presence or absence of microbial cell wall components such as LPS. We hypothesize that D-lactate exposure causes higher transcript levels of inflammatory genes, higher NO production and higher NLRP3 inflammasome activation indicated by increased IL-1β release from macrophages compared to L-lactate. We hypothesize that co-treatment with D-lactate and L-lactate

mitigates L-lactate-induced suppression of inflammatory responses in macrophages exposed to LPS.

2.3 Research aims

Using RAW 264.7 macrophage cells and primary mouse macrophages, our research objectives were:

1) To determine if D-lactate alters the transcript levels of genes involved in inflammation compared to L-lactate.
2) To characterize the effect of D-lactate versus L-lactate on inflammatory pathways and mediators, including NO and the NLRP3 inflammasome

3.0 EXPERIMENTAL METHODOLOGY

3.1 Reagents and antibodies

For a full list of reagents and antibodies used in experiments, please refer to the details contained in Table 1 and Table 2.

Table 1. Reagents used in the studies.

Reagent	Manufacturer	Reagent	Manufacturer
10X PCR Gold buffer	Applied Biosystem	HCl	Caledon
3-OBA	sigma	HEK-Blue Detection,	Invivogen
5X SSIV buffer	Invitrogen	HEK-Blue Selection	Invivogen
Amplitaq Gold	Applied Biosystem	HEPES	sigma
Anhydrous Ethanol	Fisher Scientific, Commercial Alcohol	Homogenizer ceramic beads	Omni International
Antibiotic-Antimycotic Solution 100x	Wisent Bio Product	Interferon-gamma	R&D systems
ATP	Invivogen	Isopropanol	VWR
BSA	Bioshop	LPS-*E. coli*	Invivogen
Chloroform	Anachemia	M-CSF	R&D systems
Collagenase type II	sigma	Methanol	VWR
Dithiothreitol (DTT)	Invitrogen	MgCl2	Applied Biosystem
DMEM (low glucose)	Wisent Bio Product	Molecular grade water	Mediatech
DMEM/F12	Wisent Bio Product	NaCl	Bioshop
DNAse I 10x Reaction buffer	Invitrogen	Nigericin	
DNAse I Amplification grade	Invitrogen	Normocin	Invivogen
dNTP (dATP, dTTP, dGTP, dCTP)	Wisent Bio Product	Oligo-dt(18)	McMaster Mobix Lab
EDTA	Sigma	Oligonucleotide primer	McMaster Mobix Lab
EGTA	Bioshop	PBS	Thermo Fisher
Fetal bovine serum	Wisent Bio Product	Penicillin/streptomycin	Wisent Bio Product
GlutaMAX	Thermo Fisher	Pierce LAL Chromogenic Endotoxin Quantification Kit	Thermo Fisher

GM-CSF	R&D systems	Random hexamers	McMaster Mobix Lab
Griess Reagent Kit	Invitrogen	Random pentadecamers	McMaster Mobix Lab

Table 2. Antibodies used in the studies.

Primary antibody	Catalogue number	Manufacturer
IL-6	DY406	R&D systems
CXCL-1	DY453-05	R&D systems
IL-1β	DY401	R&D systems

3.2 Cell culture

3.2.1 RAW 264.7

RAW 264.7 macrophages, courteously gifted to us from the Bowdish lab, were cultured in Dulbecco's modified eagle medium (DMEM) containing 4.5 g/L glucose, 10% heat-inactivated fetal bovine serum (FBS) and 1% penicillin/streptomycin (P/S). RAW 264.7 cells were washed with phosphate-buffered saline (PBS), then treated with low-glucose (1 g/L) DMEM containing 0.5% FBS and 1% P/S for 24 h with and without lactate and stimulated with LPS (at various doses, as indicated) for the last 4 h of treatment.

3.2.2 Primary mouse macrophage culture and differentiation

Bone marrow was harvested from the femur and tibia of 20-24-week-old C57BL/6N male mice. Mice were euthanized by cervical dislocation and bone marrow was extracted under sterile conditions. BMDMs were cultured for 7 days in DMEM containing 10% FBS, 1% P/S and 15% L929 conditioned media. For initial BMDM experiments, on day 3, media was supplemented with 75 µL L929

conditioned media. On day 7, BMDMs were treated with low-glucose (1 g/L) DMEM containing 0.5% FBS and 1% P/S for 24 h with and without lactate and stimulated with LPS (at various doses, as indicated) for the last 4 h of treatment.

The protocol for culture and differentiation of BMDMs for nitric oxide production and other experiments where indicated was adapted from Bailey *et al*.[81]. Bone marrow was harvested from the femur and tibia of 20-24-week-old C57BL/6N male mice, as previously described. On day 0, 250,000 cells/well were seeded into 24-well plates in 500 µL of phenol red-free Dulbecco's modified eagle medium/nutrient mixture F12 (DMEM/F-12) macrophage colony-stimulating factor (M-CSF) growth media containing 5% FBS, M-CSF (25 ng/mL), 1% P/S, 1% GlutaMax. Cells were cultured for 7 days, with the addition of 250 µL of phenol red-free DMEM/F12 M-CSF growth media containing M-CSF (50 ng/mL) on day 5, and the addition of granulocyte-macrophage colony-stimulating factor (GM-CSF) (50 ng/mL) on day 6. BMDMs were treated with phenol red-free DMEM/F12 containing 1% GlutaMax, 1% P/S, 2% FBS, M-CSF (25 ng/mL) and GM-CSF (50 ng/mL). Cells were treated with and without D-lactate or L-lactate for 24 h and stimulated with LPS (100 ng/mL) and IFN-γ (10 ng/mL) for 16 h.

3.2.3 HEK-293T cell culture

Human embryonic kidney (HEK-293T) cells were thawed in growth media (DMEM, 4.5 g/L glucose, 10% (v/v) FBS, 100 U/mL penicillin, 100 µg/mL streptomycin, 100 µg/mL normocin, 2 mM GlutaMax) and passaged 1:10 every 2-3 days in selection media which consisted of growth media supplemented with

1X HEK-Blue selection reagent to select for cells containing the secreted embryonic alkaline phosphatase (SEAP) promoter. Selection media for HEK-NOD1 cells contains Growth Media supplemented with 30 µg/mL blasticidin and 100 µg/mL zeocin. Passages 7-10 were used for experiments. HEK-293T cells were treated in 96-wells plates (20,000 cells/well) with and without lactate and LPS (HEK-TLR4) or FK565 (HEK-NOD1) for 24 h in Detection Media containing a SEAP colour substrate that when hydrolyzed by SEAP, produces a purple/blue colour measured at 630 nm.

3.3 Gene expression analysis

3.3.1 RNA extraction

Approximately 100,000-250,000 cells were collected in 0.3 mL TRIzol®. For all samples, 100 µL of chloroform was added and samples were mixed well and incubated at room temperature for three minutes. Each sample was then centrifuged at 12,000 x g for 10 minutes at 4 ºC. The upper aqueous phase was transferred into a fresh tube containing 150 µL isopropanol to precipitate RNA. The samples were mixed well by inverting, incubated at room temperature for 20 minutes, and then centrifuged at 12,000 x g for 10 minutes at 4 ºC. The supernatant was discarded, and the RNA pellet was washed twice with 75% ethanol. The pellet was spun down after each wash at 16,000 x g for 5 minutes at 4 ºC. Following the last wash, the remaining ethanol was evaporated before dissolving the RNA pellet in UltraPure distilled water that was pre-heated to 55 ºC. Samples were incubated at 55 ºC for 15 minutes using a VWR Hybridization

Oven. RNA concentration was measured by spectrophotometry, using Biotek Nanodrop Synergy H4 Hybrid Reader. The RNA content of each sample was equalized to 50-250 ng/µL with UltraPure distilled water and stored at -80 ºC.

3.3.2 cDNA synthesis

For each sample, 200 ng-1 µg of the RNA was mixed with 0.5 µL of DNAse I 10x Reaction buffer and 0.5 µL of Amplification grade DNAse I for 15 minutes at room temperature to eliminate single- and double-stranded DNA. Subsequently, 0.5 µL of EDTA (25mM), 0.5 µL of dNTP (10mM) and 0.5 µL of random hexamer primer (250 ng) were added to each sample. The sample was incubated in the SimpliAmp Thermal Cycler (Applied Biosystems) at 95 ºC for 10 minutes to inactivate DNAse I and 55 ºC for 10 minutes to anneal the complementary deoxyribonucleic acid (cDNA) synthesis primer. cDNA was synthesized by adding 2 µL of 5X SuperScript™ IV buffer, 0.5 µL of DTT (0.1M), 0.5 µL of UltraPure distilled water and 0.5 µL of Superscript™ IV to each sample. Each sample was incubated in the Thermal Cycler at 55 ºC for 10 minutes and 80 ºC for 10 minutes. cDNA was diluted 1:24 in UltraPure distilled water and stored at -20 ºC for all samples.

3.3.3 RT-PCR Reactions

For real-time polymerase chain reaction (RT-PCR), 10 µL of each diluted cDNA sample was mixed with 10 µL of the master mix (consisting of 5.1 µL UltraPure water, 2 µL 10X PCR Gold buffer, 2 µL $MgCl_2$, 0.4 µL dNTP (10 mM),

0.1 µL AmpliTaq® Gold and 0.4 µL primer). For a full list of commercial TaqMan primers used, refer to Table 3. RT-PCR was performed using Rotor-Gene Q (Qiagen), at 95ºC for 10 seconds, then 58 ºC for 45 seconds for 40 cycles. All genes were normalized to the average of housekeeping genes *Rn18S* and *Rplp0* using the $2^{-\Delta\Delta CT}$ method, using the experimental condition with no lactate and no LPS as the control condition.

Table 3. Primers used in RT-PCR

Primer	Gene	Catalogue Number	Manufacturer
Rn18S	Rn18S	Mm03928990_g1	ThermoFisher
Rplp0	Rplp0	Mm01974474_gH	ThermoFisher
Il6	Interleukin 6	Mmm00446190	ThermoFisher
Il1β	Interleukin 1 beta	mm00434228	ThermoFisher
Il18	Interleukin 18	Mm00600311_m1	ThermoFisher
Ccl2	Chemokine (C-C motif) ligand 2	mm00441242	ThermoFisher
Nos2	Nitric oxide synthase 2, inducible	mm00440502	ThermoFisher
Il23	Interleukin 23	mm01160011	ThermoFisher
Cd40	CD40 antigen	mm00441891	ThermoFisher
Tnf	Tumour necrosis factor	mm00443258	ThermoFisher
Il10	Interleukin 10	mm00439616	ThermoFisher
Il1rn	Interleukin 1 receptor antagonist	mm00446186	ThermoFisher
Cxcl10	chemokine (C-X-C motif) ligand 10	mm00445235	ThermoFisher

3.4 Cytokine release

DuoSet enzyme-linked immunosorbent assays (ELISA) (R&D Systems) were used to measure IL-6 and CXCL-1 in the media of BMDMs plated at 2.5 x

10^5 cells/well in a 24-well plate on days 7-10 of culture treated with and without lactate and LPS for 24 h or 48 h.

3.5. Nitric oxide quantification

NO production in cultured media of BMDMs was quantified by measuring nitrite levels, a stable breakdown product of NO. Cell culture media from BMDMs was collected after 24 h. In a 96-well plate, 150 µL nitrite-containing sample, 130 µL deionized water and 20 uL Griess reagent containing 1:1 N-(1-naphthyl)ethylenediamine dihydrochloride 1 mg/mL and sulfanilic acid (10 mg/mL) were incubated at room temperature for 30 min. The absorbance of the nitrite-containing samples was measured relative to the reference sample in a spectrophotometer microplate reader at a wavelength of 548 nm.

3.6 Quantification of gram-negative bacterial endotoxins

Levels of gram-negative bacterial endotoxins were determined by measuring p-Nitroaniline release proportional to the activation of proenzyme Limulus Amebocyte Lysate by bacterial endotoxins. In a 96-well plate, 50 µL of sample, 50 µL of LAL reagent, and 100 µL of chromogenic substrate were incubated for 10 minutes at 37°C. To stop the reaction, 100 µL of 25% acetic acid was added to the plate. The absorbance of the endotoxin-containing samples was measured relative to the reference sample in a spectrophotometer microplate reader at a wavelength of 405-410 nm.

3.7 Statistical analyses

Statistical analyses were carried out using Prism 9.0 software. Normality was determined using the D'Agostino-Pearson test. Two-tailed unpaired, nonparametric Mann-Whitney tests were used to determine the differences between two groups when data were not normally distributed. Two-tailed unpaired, parametric t-tests were used between two groups when the data were normally distributed. Kruskal-Wallis tests were used between multiple means when the data were not normally distributed. One-way analysis of variance (ANOVA) was used to determine differences among three groups for normally distributed data. Two-way ANOVA with Fisher's LSD test was used to determine significant interaction between multiple means for normally distributed data so that each comparison stands alone when comparing between conditions. All results are expressed as mean ± SEM (standard error of the mean) with $p<0.05$ considered significant.

In mice, each biological replicate was defined as a separate animal. In clonal cell culture, each biological replicate was defined as a separate cell passage or separate day. In primary cell culture, each biological replicate was defined as a separate animal or separate day.

4.0 RESULTS

4.1 Effect of lactate on media pH and endotoxin contaminants

First, we determined whether physiological levels of D-lactate or L-lactate would alter the pH or be a source of endotoxin in cell culture. We compared changes in pH of (i) high-dose physiological D-lactate (100 µM), (ii) equimolar L-lactate (100 µM), (iii) physiological L-lactate (5 mM) and (iv) physiological D-lactate and L-lactate (D-lactate 100 µM + L-lactate 5 mM) to (NaCl 5 mM). In low-glucose DMEM with 5% FBS, 1% P/S and 1% GlutaMax, all doses of lactate did not alter the pH of the media (Figure 3A). We also measured endotoxin units in lactate-containing media to determine levels of endotoxin contaminants. Levels of endotoxin units/mL (EU/mL) in low-glucose DMEM with L-lactate or D-lactate were less than 0.1 EU/mL which is comparable to those found in the endotoxin-free water control (Figure 3B).

4.2 Transcript levels of inflammatory genes in mice colonized with high and low microbial producers of D-lactate

We aimed to test whether D-lactate alters inflammation differently than L-lactate in the livers and adipose tissue of mice. Preliminary data collected by lab member Dr. Anhê showed that *L. intestinalis* produces 400x more D-lactate than *L. reuteri* (Figure 4A), and then colonized germ-free mice with D-lactate^{HI} (*L. intestinalis*) or D-lactate^{LO} (*L. reuteri*)-producing microbiota (Figure 4B). We measured inflammatory gene expression in liver tissue of D-lactate^{HI} vs D-lactate^{LO}-colonized mice. Transcript levels of *Il1β* and *Il18* in the liver were

significantly higher in mice colonized with D-lactate^{HI} microbiota compared to mice colonized with D-lactate^{LO} microbiota (Figure 5A). Similarly in the adipose tissue, transcript levels of *Ccl2* were significantly higher after colonization with D-lactate^{HI} microbiota compared to mice colonized with D-lactate^{LO} microbiota (Figure 5B). Overall, colonization of mice with bacteria that are high D-lactate producers increased the expression of genes involved in liver and adipose tissue inflammation.

4.3 Lactate alters transcripts related to inflammation in RAW 264.7 macrophages

Since transcript levels of genes involved in innate immunity were increased in response to high D-lactate-producing gut bacteria *in vivo*, we next compared physiological and equimolar D-lactate and L-lactate in RAW 264.7 macrophages to determine the role of D-lactate in inflammatory gene expression in a cell-autonomous model. Cells were treated with D-lactate (25 µM, 100 µM) or L-lactate (25 µM, 100 µM, 1 mM) for 24 h and stimulated with TLR4 ligand, *E. coli*-derived LPS (0, 0.2, 2, 20 ng/mL) for the last 4 h (Figure 6).

Others showed treatment of BMDMs with lactate by itself did not alter pro-inflammatory gene expression, and that stimulation with LPS was required[70]. Similarly, we showed in RAW 264.7 macrophages that most inflammatory gene expression was either undetected or unaltered by D-lactate or L-lactate without LPS (not shown). In LPS-stimulated RAW 264.7 macrophages, the effects of L-lactate and D-lactate on inflammatory gene expression were complex and differed between each cytokine (Figure 7A-I). The expression of *Il23* (Figure 7C),

Tnf (Figure 7E), *Il18* (Figure 7F), *Il10* (Figure 7G) and *Ccl2* (Figure 7I) did not change in response to physiological or equimolar D-lactate or L-lactate in LPS-stimulated RAW 264.7 macrophages. However, transcript levels of *Il6* (Figure 7A), *Il1β* (Figure 7B), *Cd40* (Figure 7D), and *Nos2* (Figure 7H) were significantly lower in response to 25 µM L-lactate, but not equimolar D-lactate (25 µM). In addition, we found that all doses of D-lactate and L-lactate significantly lowered *Nos2* expression in response to LPS (20 ng/mL) (Figure 5H). However, physiological L-lactate (1 mM) lowers LPS-induced *Nos2* expression more than physiological D-lactate (100 µM), suggesting that D-lactate may be more pro-inflammatory than L-lactate at physiological levels *in vitro*. Further, low dose equimolar L-lactate (25 µM), lowered LPS-induced *Nos2* expression more than equimolar D-lactate (25 µM) (Figure 7H).

4.3.1 D-Lactate and L-lactate in combination alter transcripts related to inflammation in RAW 264.7 macrophages

Next, we tested the effect of physiological D-lactate (25 µM - 100 µM) in the presence of physiological L-lactate (1 mM) on inflammatory gene expression in RAW 264.7 macrophages. This is important because tissues and cells would be exposed to both L-lactate and D-lactate *in vivo*. Cells were treated with physiological L-lactate (1 mM) and physiological D-lactate (25 µM or 100 µM) for 24 h and stimulated with LPS (20 ng/mL) for the last 4 h (Figure 6). We observed that in the presence of L-lactate, physiological levels of D-lactate did not alter the

expression of most inflammatory genes in macrophages (Figure 8A, B, E, F, I). In response to D-lactate (25 µM) + L-lactate (1 mM), transcript levels of the anti-inflammatory cytokine *Il10* are significantly lower compared to the control (Figure 8G). However, *Il23* (Figure 8C) and *Cd40* (Figure 8D) expression is significantly higher after D-lactate (100 µM) + L-lactate (1 mM) compared to 1 mM L-lactate alone. Further, increasing D-lactate from 25 µM to 100 µM in the presence of 1 mM L-lactate significantly increased *Nos2* expression in response to LPS (Figure 8H).

4.4 Inflammatory transcript levels in primary mouse hepatocytes in response to lactate

Others have shown that D-lactate alters hepatic inflammation by modulating the Kupffer cell response to pathogens[29]. However, it was not clear if hepatocytes would have different inflammatory signatures after exposure to D-lactate versus L-lactate. To determine the role of D-lactate on hepatic inflammation *in vitro*, we compared the effect of D-lactate (25 µM, 100 µM) to equimolar and physiological L-lactate (25 µM, 100 µM, 1 mM) on inflammatory gene expression in primary hepatocytes stimulated with LPS (0.2, 2, 20 ng/mL) (Figure 9). Similar to our findings in RAW 264.7 macrophages, the relationship between lactate and cell-autonomous inflammation was complex. Physiological concentrations of D-lactate promoted less inflammation than L-lactate in primary mouse hepatocytes (Figure 10). Specifically, expression of *Il1β* (Figure 10A)*, Il23*

(Figure 10B) and *Cd40* (Figure 10C) were significantly lower in response to D-lactate (25 µM, 100 µM) compared to L-lactate (25 µM, 100 µM, 1mM).

4.5 Effect of lactate on TLR4-mediated and NOD1-mediated NF-κB activation

We next sought to characterize the inflammatory pathways involved in lactate-mediated modulation of the inflammatory response. We first explored the effect of D-lactate and L-lactate on TLR4-mediated NF-κB activation using the HEK-293T reporter cells (Figure 11). We tested 24 h exposure to D-lactate vs L-lactate in HEK-293T cells that overexpress TLR4 combined with 2 ng/mL LPS (Figure 12A) or 0.5 ng/mL LPS (Figure 12B). In response to 0.5 ng/mL or 2 ng/mL LPS, we did not detect differences in NF-κB activation in response to increasing D-lactate or L-lactate concentrations (Figure 12A-B). We also tested the effect of LPS (2 ng/mL) plus physiological D-lactate (25 µM - 100 µM) in the presence of physiological L-lactate (1 mM) on NF- κB activation in HEK-TLR4 cells (Figure 12C). L-lactate at 1 mM significantly increased NF-κB activation relative to the LPS-only group. However, the addition of 25 µM or 100 µM D-lactate did not alter LPS-mediated NF- κB activation in this assay.

In addition, we tested the effect of D-lactate and L-lactate on NOD1-mediated NF-κB activation using the HEK-293T assay (Figure 11). We tested 24 h exposure to D-lactate vs L-lactate in HEK-293T cells that overexpress NOD1 stimulated with the synthetic NOD1 ligand FK565 at 100 ng/mL (Figure 13A). In response to a NOD1 ligand, physiological D-lactate (100 µM) significantly increased NF-κB activation compared to 1 mM L-lactate (Figure 13A). In the

presence of physiological L-lactate (1 mM), the addition of 25 µM or 100 µM D-lactate did not alter NOD1-mediated NF- κB activation in this assay (Figure 13B).

4.6 IL-6 release in primary macrophages during endotoxin exposure in response to lactate

As previously shown, D-lactate increased NF-κB activation in HEK-293T NOD1 cells compared to L-lactate (Figure 7), which favours the downstream production of pro-inflammatory cytokines such as IL-6. We measured IL-6 release from primary macrophages in response to D-lactate and L-lactate during endotoxin exposure. Primary macrophages were treated with D-lactate (25 µM, 100 µM, 1 mM), L-lactate (25 µM, 100 µM, 1 mM) or D-lactate in the presence of L-lactate (L-lactate 1 mM + D-lactate 25 µM, L-lactate 1 mM + D-lactate 100 µM) and stimulated with NOD1 ligand (FK565) or TLR4 ligand (LPS) (Figure 14A). IL-6 release was measured after 48 h by enzyme-linked immunosorbent assay (ELISA).

In primary macrophages, 1 mM L-lactate significantly reduced IL-6 levels compared to the control condition in BMDMs stimulated with LPS (200 ng/mL) (Figure 15). Further, LPS-induced (200 ng/mL) IL-6 release increased in response to physiological D-lactate (100 µM) compared to L-lactate (1 mM) after 48 h (Figure 15). Adding 1 mM L-lactate to 100 µM D-lactate significantly reduced IL-6 secretion from 100 µM D-lactate alone in BMDMs stimulated with LPS (200 ng/mL) (Figure 15). Previously, we showed that D-lactate in the presence of L-lactate did not increase NF-κB activation in HEK-293T cells in

response to TLR4 to NOD1 ligands (Figure 12-13). Similarly, in the presence of L-lactate, D-lactate (25 µM and 100 µM) did not increase IL-6 release in response to TLR4 or NOD1 ligands (Figure 15).

4.7 NLRP3 inflammasome effector levels during endotoxin exposure in response to lactate

As mentioned, transcript levels of *Il1β* and *Il18* increased in liver tissue of mice colonized with bacteria that high D-lactate-producing bacteria versus low levels of D-lactate, which are downstream products of NLRP3 inflammasome activation (Figure 5). We tested whether D-lactate and L-lactate alter NLRP3 inflammasome activation in primary macrophages. BMDMs were differentiated using L929 conditioned media for 7 days (Figure 14A). Primary macrophages were treated with D-lactate (25 µM, 100 µM, 1 mM), L-lactate (25 µM, 100 µM, 1 mM) or D-lactate in the presence of L-lactate (L-lactate 1 mM + D-lactate 25 µM, L-lactate 1 mM + D-lactate 100 µM) for 24 h and stimulated with 200 ng/mL LPS and nigericin (20 µM) for 30 min or ATP (2.5 ng/mL) for 1 h. Levels of secreted IL-1β in the media were measured by ELISA as an indicator of NLRP3 inflammasome activation.

In LPS-primed BMDMs, physiological L-lactate (1 mM) significantly reduced nigericin-induced inflammasome-mediated IL-1β release compared to control (Figure 16A). However, equimolar D-lactate (1 mM) did not suppress IL-1β release compared to the control condition in LPS-primed BMDMs, rather equimolar D-lactate (1 mM) increased nigericin-induced and ATP-induced IL-1β

production compared to L-lactate (1 mM) (Figure 16A). This finding shows that D-lactate alters NLRP3 inflammasome activation compared to L-lactate in macrophages.

Further, physiological D-lactate (100 µM) increases nigericin-induced IL-1β release in LPS-primed BMDMs compared to physiological L-lactate (1 mM) despite the 10-fold differences in the dose of lactate. Next, we treated LPS-primed BMDMs with physiological levels of D-lactate plus L-lactate which reflects the physiological environment where both enantiomers are present together. In the presence of L-lactate (1 mM), D-lactate (25 µM and 100 µM) prevented L-lactate lowering of nigericin-induced and ATP-induced IL-1β release (Figure 16A). Therefore, the presence of a physiological dose of D-lactate prevented lower NLRP3 inflammasome-mediated IL-1β release caused by physiological L-lactate in response to a TLR4 ligand and known NLRP3 inflammasome activators in primary mammalian macrophages.

IL-6 is a pro-inflammatory cytokine that is not regulated by the NLRP3 inflammasome. We aimed to determine whether lactate alters IL-6 release in response to NLRP3 inflammasome activators nigericin or ATP during endotoxin exposure. Our results showed that lactate modulates IL-6 release in a similar manner to IL-1β and that D-lactate is more pro-inflammatory than L-lactate for both cytokines. In LPS-primed BMDMs, physiological L-lactate (1 mM) significantly lowered nigericin-induced and ATP-induced IL-6 secretion compared to the control condition (Figure 16B). Again, equimolar D-lactate (1 mM) did not

suppress IL-6 secretion, rather D-lactate (1 mM) increased IL-6 production compared to L-lactate (1 mM) in LPS primed BMDMs treated with nigericin or ATP (Figure 16B). Physiological D-lactate (100 µM) increased IL-6 release in LPS-primed BMDMs compared to physiological L-lactate (1 mM) after nigericin or ATP treatment (Figure 16B). In the presence of L-lactate (1 mM), D-lactate (25 µM and 100 µM) prevented L-lactate lowering of IL-6 release in LPS-primed BMDMs treated with nigericin or ATP (Figure 16B). These findings show that compared to L-lactate, D-lactate generates a higher inflammatory response for an NLRP3 inflammasome-mediated cytokine (IL-1β), and a cytokine not processed through this inflammasome (IL-6). Further, the presence of a physiological dose of D-lactate prevented reduced NLRP3 inflammasome-mediated IL-1β and IL-6 release caused by physiological L-lactate in response to known NLRP3 inflammasome activators in LPS-primed macrophages.

4.8 NO production in primary macrophages during exposure to TLR4 and NOD1 ligands and lactate

Our previous work showed that L-lactate lowers LPS-induced *Nos2* expression more than D-lactate in RAW 264.7 macrophages (Figure 7H). Inducible nitric oxide synthase (iNOS) that is encoded by the *Nos*2 gene is central to inflammatory macrophage polarization and function and generates nitric oxide upon activation with LPS and IFN-γ[82]. Increased *Nos2* expression and higher NO production are biomarkers of M1 macrophage polarization, which is typical of a higher inflammatory status. Hence, we next compared the effect of

physiological and equimolar D-lactate and L-lactate during TLR4-mediated inflammation on NO production in primary bone marrow-derived macrophage (BMDM) culture. We also built on our work showing that co-stimulation with other inflammatory factors such as LPS priming plus nigericin can alter the D-lactate versus L-lactate response in BMDMs compared to LPS alone. BMDMs were differentiated by the Bailey *et al*. protocol using recombinant macrophage colony-stimulating factors and co-stimulated with IFN-γ (Figure 14B)[81]. These BMDMs were treated with D-lactate (25 µM, 100 µM, 1 mM), L-lactate (25 µM, 100 µM, 1 mM) or D-lactate in the presence of L-lactate (L-lactate 1 mM + D-lactate 25 µM, L-lactate 1 mM + D-lactate 100 µM) for 24 h and stimulated with TLR4 ligand LPS (derived from *E. coli*) and IFN-γ (10 ng/mL) or the NOD1 ligand FK565 (10 µg/mL) and IFN-γ (10 ng/mL) for 16 h[81]. Nitrite content in the media was measured using Griess assay as an indicator of NO production.

In IFN-γ co-stimulated BMDMs, physiological L-lactate (1 mM) significantly suppressed NO production compared to vehicle control in response to LPS (2 ng/mL or 200 ng/mL) or FK565 (10 µg/mL) (Figure 17A). However, equimolar D-lactate (1 mM) did not suppress NO production and increased NO production compared to L-lactate (1 mM) in IFN-γ co-stimulated BMDMs stimulated with LPS (2 ng/mL or 200 ng/mL) or FK565 (10 µg/mL) (Figure 17A). This finding shows that D-lactate and L-lactate when compared at equal doses, alter inflammation and macrophage activation differently, where D-lactate promotes cell-autonomous NO-mediated inflammation in macrophages.

Importantly, our data also shows that physiological D-lactate (100 µM) increases NO production compared to physiological L-lactate (1 mM) in IFN-γ co-stimulated BMDMs despite the 10-fold differences in the lactate dose (Figure 17A). Again, we treated primary macrophages with physiological levels of D-lactate in the presence of L-lactate which reflects the physiological environment where both enantiomers are present together. In the presence of L-lactate (1 mM), D-lactate (25 µM and 100 µM) prevented the ability of L-lactate to lower NO production in IFN-γ co-stimulated BMDMs (Figure 17A). Therefore, a physiological dose of D-lactate prevented lower NO production mediated by physiological L-lactate in response to multiple bacterial ligands including TLR4 and NOD1 activators.

4.9 Comparison of primary macrophage differentiation and culture methods on lactate-mediated effects on IL-6 release, and whether co-stimulation is required

We previously showed that 1 mM L-lactate 1 significantly reduced IL-6 compared to the control and 100 µM D-lactate, but that physiological levels of D-lactate were not sufficient to impair suppression of inflammation by L-lactate (Figure 15). However, in BMDMs treated with NLRP3 activators, the addition of physiological D-lactate prevented L-lactate-induced lowering of IL-6 release (Figure 16B). Similarly, D-lactate prevented L-lactate-induced lowering of NO which occurred in BMDMs differentiated with M-CSF and GM-CSF and co-stimulated with IFN-γ (Figure 17B) Therefore, we aimed to determine whether BMDM differentiation using recombinant macrophage colony-stimulating factors

and IFN-γ co-stimulation may reveal lactate-mediated effects on inflammation, such as IL-6 secretion. Using this method of activating macrophages, we measured IL-6 release from BMDMs differentiated using the method published by Bailey *et al*. Figure 14B). During LPS exposure (2 ng/mL and 200 ng/mL) and co-stimulation with IFN-γ (10 ng/mL), L-lactate treatment at 1 mM significantly lowered IL-6 release (Figure 17B). At LPS 2 ng/mL and 200 ng/mL, physiological D-lactate (100 µM) increased IL-6 release compared to L-lactate 1 mM (Figure 17B). Again, adding physiological D-lactate (25 µM or 100 µM) in the presence of L-lactate 1 mM was sufficient to significantly increase IL-6 release compared to L-lactate 1 mM alone (Figure 17B). These data show that co-stimulation with IFN-γ and/or differentiation using recombinant macrophage colony-stimulating factors programs primary macrophages to generate more inflammation in response to D-lactate versus L-lactate.

4.10 Effect of lactate transporter inhibition on NO production in primary macrophages during exposure to TLR4 and NOD1 ligands and lactate

We aimed to determine whether cellular transport of lactate was required for changes in NO production in macrophages. BMDMs were differentiated using the Bailey *et al*. method optimized for NO production and co-stimulated with IFN-γ (Figure 14B)[81]. Macrophages were treated with 1 mM NaCl as a control or 1 mM L-lactate and lactate transporter inhibitor α-Cyano-4-hydroxycinnamic acid (αCHC) (0.5-7.5 mM) (Figure18A) or 3-hydroxy-butyrate acid (3-OBA) (0.3-5 mM)

(Figure 18B) for 24 h. Indicated groups were stimulated with LPS (200 ng/mL) and IFN-γ (10 ng/mL) for 16 h.

In the presence of L-lactate 1 mM, αCHC suppressed nitrite release in BMDMs (Figure 18A). However, in the absence of L-lactate 1 mM, αCHC also decreases nitrite levels dose-dependently (Figure 18A). In the absence of 1 mM L-lactate, 3-OBA (0.3-5 mM) did not alter nitrite release compared to the LPS-only group. However, 3-OBA also did not alter (increase) nitrite suppression by 1 mM L-lactate. These data show that αCHC and 3-OBA are not suitable chemical inhibitors to study D-lactate versus L-lactate transport inhibition. The inhibitor αCHC has effects on NO in the absence of any lactate and 3-OBA did not alter L-lactate mediated inflammation, and it is debated if 3-OBA even inhibits lactate transport[83].

5.0 DISCUSSION

Many studies have investigated the metabolic basis of diseases such as type 2 diabetes and NAFLD. One emerging aspect is the connection between metabolism and immunity, where metabolic intermediates can alter tissue or cell-specific immune responses. The Cori cycle was first described in 1929, and the role of lactate in host metabolism and health has been extensively researched. Lactic acid is a product of anaerobic glycolysis which is favoured in low-oxygen and low-glucose environments[71,84]. Lactate buildup in tissues is characteristic of inflammation and cancer, but recent research shows that lactate is more than just a biomarker of disease, but rather lactate engages as a bioactive molecule that can modulate immune responses[71]. Given that lactate is a key substrate in host glucose synthesis and metabolism, understanding its capacity to alter both inflammation and metabolism relating to metabolic disease is imperative. Microbial dysbiosis is known to exacerbate metabolic disease and comparing how host-derived L-lactate and microbial-derived D-lactate alter inflammation differently may identify mechanisms by which gut microbiota impact aspects of host immunity such as metabolic inflammation.

A lot of published research does not distinguish between the use or investigation of L-lactate versus D-lactate. Some studies have shown that L-lactate or racemic lactate suppresses pro-inflammatory responses, while others suggest that lactate exacerbates the inflammatory response. Errea *et al*. found that lactate inhibited GPR81-mediated inflammatory signalling in macrophages

by abrogating LPS-induced expression of pro-inflammatory cytokines IL-6, CD40 and IL12p40[70]. Others have similarly shown that lactate promotes M2 polarization of macrophages[85,86]. Importantly, the aforementioned studies focus on L-lactate or racemic D-/L-lactate. On the contrary, D-lactate can promote pro-inflammatory macrophage-mediated immune responses in the liver, although the mechanism by which this microbial metabolite elicits this immunogenic effect remains unknown[29]. It was also unknown if D-lactate can increase cell-autonomous immune responses in hepatocytes or macrophages. We have previously shown that reducing intestinal absorption of microbial D-lactate decreases blood glucose and mitigates insulin resistance in obese mice (Unpublished, 2020). The impact of D-lactate on mechanisms of metabolic disease such as metabolic inflammation is largely unknown. Understanding how D-lactate alters cell-autonomous immunity in macrophages and hepatocytes is positioned to increase our knowledge about how microbes can confer metabolic inflammation to the liver, which is relevant to blood glucose control and NAFLD. This is a key knowledge gap since levels of D-lactate and L-lactate are elevated in T2D patients' urine and plasma[58]. When assessing cell-autonomous immunity, it was critical to determine the effect of D-lactate at physiological doses and in combination with L-lactate and other microbial components that engage innate immunity and the consequent effects on macrophage inflammation.

5.1 L-lactate lowers inflammatory gene expression in macrophages

Identifying the role of D-lactate in macrophage programming and activation may further our understanding of how D-lactate can promote insulin resistance and the progression of NAFLD. We sought to fill this knowledge gap and compare the effect of D-lactate vs L-lactate on inflammation in macrophages.

We first used an *in vitro* RAW 264.7 macrophage model to screen multiple inflammatory mediators at the transcript level. As previously observed by Errea *et al*.,[70] we showed that D-lactate or L-lactate alone does not augment or alter pro-inflammatory gene expression. Lactate is a non-immunogenic metabolite and there is no known immune receptor. However, metabolites can co-operate with known immunogenic ligands to alter immune responses. For example, SCFAs are also bacteria-derived metabolites that are not known to directly engage immune receptors but are still important modulators of inflammatory responses by altering immune responses in concert with immunogenic microbial components[62,63]. Therefore, we hypothesized that when combined with a microbial component that engages immunity such as a TLR4 or NOD1 ligand, D-lactate would alter immune responses differently than L-lactate. Hence, we compared D-lactate vs L-lactate stimulated with low doses of the TLR4 ligand LPS. We observed that physiological levels of D-lactate increased specific markers of inflammation (i.e., *Nos2*) compared to physiological L-lactate, at doses reflective of the *in vivo* systemic blood environment. These findings show

that although D-lactate or L-lactate do not augment the net inflammatory response through synergy with TLR4 agonists such as LPS, the enantiomers play different roles in modulating innate immunity where L-lactate promotes less inflammation than D-lactate.

To better reflect the physiological environment, we explored whether the combination of physiological doses of both L-lactate and D-lactate alters inflammation. In RAW 264.7 macrophages, we found that *Nos2* expression significantly increased when, in the presence of 1 mM L-lactate, D-lactate is increased from 25 µM to 100 µM. This data further suggests that D-lactate is more pro-inflammatory than L-lactate, and D-lactate alters inflammation in the presence of L-lactate reflective of the physiological environment. In particular, increasing D-lactate from the lower part of the physiological range (25 µM) in the blood to the upper physiological range (100 µM) increases *Nos2* even in the presence of 1 mM L-lactate. This is an important result because it shows that altering D-lactate in the micromolar range can affect immune responses despite L-lactate presence in millimolar concentrations.

5.2 D-lactate promotes NO production in activated macrophages

We have shown that D-lactate alters inflammation differently than L-lactate in a cell-autonomous model, adding to recently published work showing that microbial-derived D-lactate from the gut altered immunity in the liver by programming tissue-resident macrophages to clear a bacterial infection[29]. It is

unknown through which signalling pathways D-lactate modulates immune responses, particularly in macrophages.

We sought to characterize the inflammatory pathways modulated by lactate. Our results suggested that D-lactate may influence macrophage programming via increased *Nos2* expression and NO production. We showed that physiological and equimolar D-lactate significantly increased NO production and rescued suppressed NO production by L-lactate in primary macrophages derived from mice. Combining physiological levels of L-lactate and D-lactate *in vitro* models the *in vivo* physiological environment where both enantiomers are present and act on macrophages. BMDMs were also classically activated by LPS and IFN-γ, causing increased NO production characteristic of M1 polarization[87]. This pro-inflammatory phenotype favours the release of inflammatory cytokines such as IL-6, which we also showed increased in response to physiological levels of D-lactate compared to L-lactate. Together, these findings highlight the pro-inflammatory nature of D-lactate and the opposing effect on inflammation by L-lactate.

To confirm that extracellular L-lactate and D-lactate directly impact NO production, we tested the effect of various lactate transporter inhibitors. αCHC is a known inhibitor of MCT-1, which is a transporter responsible for lactate influx expressed on the cell membrane of macrophages[70,88,89]. MCT-1 appears to be a good target to inhibit lactate transport and alter immunity. MCT-1 transports both L-lactate and D-lactate across the cell membrane[90]. Knockdown of MCT-1

reduced LPS-induced expression of iNOS, IL-1β and IL-6 in BV2 microglial cells, which are specialized macrophages found in the CNS[91]. We tested whether αCHC would inhibit L-lactate 1 mM-induced lowering of NO production in BMDMs. We found that αCHC dose-dependently inhibited NO production in the absence of L-lactate. In addition, NO production was very low at all doses of αCHC in the presence of 1 mM L-lactate. These data show that αCHC is not a suitable chemical inhibitor to study the effect of lactate on macrophage immunity. Validation of the dose-response relationship of αCHC and D-lactate versus L-lactate cellular transport is needed. Even if this is done, αCHC may not be suitable since the chemical inhibited NO production without lactate.

GPR81 is a cell surface receptor for lactate and is involved in propagating the immunomodulatory effects of lactate[70,80,92]. 3-OBA has been widely used in the literature as a purported GPR81 inhibitor, but 3-OBA has not been validated as an antagonist of GPR81[80,93,94]. Rather, 3-OBA is an agonist of GPR109A[95]. In fact, the use of 3-OBA as a GPR81 inhibitor has been criticized by Nezhady *et al.* who also claim that there are currently no known antagonists of GPR81[83]. As expected, 3-OBA did not alter NO production in the absence of 1 mM L-lactate. However, 3-OBA did not change NO production in the presence of 1 mM L-lactate. Overall, validation of lactate transport inhibition and optimization of the dose of GPR81 and MCT-1 inhibitors are required as it is not clear if these inhibitors actually prevent lactate influx or if they have non-specific effects on NO production.

It is clear that D-lactate and L-lactate modulate macrophage inflammation differently. L-lactate promotes an anti-inflammatory response during pre-existing inflammation in classically activated macrophages. Even in the presence of L-lactate, D-lactate promotes inflammation and characteristics indicative of M1 macrophage polarization. We have identified that increased *Nos2* expression and higher NO production is one mechanism by which D-lactate programs tissue-resident macrophages.

The role of *Nos2* expression and NO production in adaptive and innate immune responses has been studied extensively. It is known that *Nos2*-mediated NO production plays a key role in host defence against bacterial infection by direct killing of pathogens[96]. Macrophage-mediated killing and phagocytosis of bacterial pathogens in the liver are dependent on reactive oxygen species production[97]. It has been shown in RAW 264.7 macrophages that induction of iNOS (*Nos2*) upregulates reactive oxygen species via protein kinase C assembly and activation of NADPH oxidase[98]. McDonald *et al.* showed that ROS-dependent pathogen capture and killing by Kupffer cells is controlled by gut microbiota[29]. These authors also found that clearance of circulating pathogens was functionally regulated by gut microbiota-derived D-lactate[29]. We have shown that D-lactate promotes NO production in activated BMDMs, which may program macrophages to clear circulating bacterial infections via ROS production. The release of a bacterial metabolite from commensals protects against infection from

a pathogen, where we identified cell-autonomous NO response as a potential mediator of this immune response.

5.3 L-lactate lowers NLRP3 inflammasome activation and IL-1β

Other than the regulation of NO defined by our results, it was not clear what immune pathways were differentially regulated by L-lactate and D-lactate. Although our results showed that physiological D-lactate (100 μM) increased NF-κB activation more than L-lactate (1 mM) in response to bacterial cell wall muropeptides acting on NOD1, the effect was very small. Further, this effect was not evident when stimulated with TLR4 ligand, LPS. Regulation of NF-κB appears not to be a key discriminator of the effects of D-lactate versus L-lactate. It is also possible that HEK-293T reporter cells used to model NF-κB activation in response to lactate are not a suitable model to study the interaction of lactate enantiomers and bacterial components.

IL-6 secretion is downstream of NF-κB activation. Given that L-lactate lowered IL-6 secretion more than D-lactate in BMDMs co-stimulated with INFγ and LPS, the role of NF-κB should be re-visited in these polarized macrophages. These results suggest that co-stimulation and polarization of macrophages may be required for observing the effects of lactate enantiomers on TLR4-mediated immune responses. The HEK-293T model may not be ideal to capture this response, which could be macrophage-specific.

We have provided *in vitro* evidence in support of D-lactate promoting inflammation more than L-lactate through NO production and IL-6 secretion.

Upon measuring inflammatory gene expression, we found that *Il1β* and *Il18* transcript levels significantly increased in liver tissue of GF mice colonized with bacteria that produced high levels of D-lactate versus low levels of D-lactate (i.e., D-lactate^{HI} compared to D-lactate^{LO} colonized mice), suggesting the involvement (or at least priming) of the NLRP3 inflammasome. During the priming step of the NLRP3 inflammasome, PRRs such as TLR4 respond to a PAMP and activate NF-κB leading to the production of pro-interleukin-1β (IL-1β) and pro-interleukin-18 (IL-18). Activation of the NLRP3 inflammasome, such as in the presence of exogenous ATP, or pore-forming toxins (such as nigericin) results in NLRP3 assembly, Caspase-1 activation, and cleavage and secretion of the bioactive forms of IL-1β and IL18.

It is not yet clear how D-lactate could increase the priming step of the NLRP3 inflammasome, which may have not been modelled well in our experiments using naive HEK293T reporter cells. Given the results in mouse livers, we assessed a role for D-lactate versus L-lactate in NLRP3 activation in LPS-primed macrophages. We compared the effect of physiological and equimolar levels of D-lactate and L-lactate in BMDMs in response to TLR4 ligand LPS and known NLRP3 inflammasome activators nigericin and ATP. Physiological levels of L-lactate (i.e., 1mM) significantly lowered IL-1β release compared to equimolar and physiological D-lactate. Equimolar D-lactate (i.e., 1 mM) did not lower IL-1β secretion in response to NLRP3 activators. Further, D-lactate prevented L-lactate-induced lowering of IL-1β. These data show that L-

lactate decreases activation of the NLRP3 inflammasome, but D-lactate generates an environment where the NLRP3 inflammasome is more active and that this can happen in a cell-autonomous manner in macrophages. If this effect was specific to the NLRP3 inflammasome then cytokines other than IL-1β (and IL-18) would respond differently to D-lactate. We found that the same effect of D-lactate induces higher inflammation compared to L-lactate for IL-6 secretion in response to NLRP3 inflammasome activators nigericin and ATP in LPS-primed macrophages. Others have shown that GPR81 activation by lactate reduces the effect of TLR4 agonists via attenuation of NF-κB and inhibition of NLRP3 inflammasome-mediated release of IL-1β[69,99]. Here, we have honed this response and discovered that the effect of lactate on NLRP3 inflammasome activation is enantiomer specific.

The ability of gut commensal bacteria to modulate immune responses in distant tissues suggests a method of long-distance communication. We have shown that TLR4 ligands and small molecule metabolites derived from gut microbiota, such as D-lactate, increase NLRP3 inflammasome-mediated IL-1β production compared to L-lactate. Further, autocrine induction of IL-1β levels also induces the production of secondary inflammatory mediators such as IL-6[100]. Following NLRP3 inflammasome-mediated inflammation, these inflammatory cytokines can exacerbate insulin resistance and promote the progression of obesity and T2D[101]. Our data shows that D-lactate, compared to L-lactate, promotes NLRP3 inflammasome-mediated IL1β production which can drive IL-6

signalling downstream which may promote insulin resistance and the progression of T2D.

5.4 Future directions

We have shown that D-lactate and L-lactate have different effects on macrophage inflammation, given specific co-stimulation and polarization signals. NO production, a key characteristic of M1 polarization, is lower in macrophages treated with L-lactate. A future direction for this work would be to determine whether D-lactate or L-lactate promote other indicators of the M1 or M2 polarization spectrum in BMDMs. One method of determining the degree of M1 vs M2 polarization is by comparing gene signatures in response to lactate by using a ratio of interleukin-12b (IL-12b)/arginase-1 gene expression, as described by others[87]. Future tests may also involve measuring M1 surface markers such as TLR4, CD80, CD86 and iNOS, and M2 surface markers CD206, CD163 and CD209[102].

Another future direction for this work is to optimize lactate transporter inhibition. Our results showed that αCHC and 3-OBA did not modulate L-lactate-induced lowering of NO production in classically activated BMDMs. An important future test would be to confirm whether αCHC and 3-OBA or other potential inhibitors are inhibiting L-lactate and D-lactate transport by measuring the cellular transport of radiolabeled D-lactate and L-lactate into BMDMs. Inhibition of lactate transport by αCHC and 3-OBA would require dose and timepoint optimization. If

αCHC and 3-OBA or another inhibitor sufficiently inhibit lactate transport, the next step would be to find a dose and time that does not independently alter NO production (ie. in the absence of L-lactate) and re-test if inhibition of lactate transport alters NO production. Another important future direction would be to delete MCT-1 and/or GPR81 and assess L-lactate and D-lactate transport and NO levels.

A recent seminal paper showed that microbial-derived D-lactate programmed hepatic Kupffer cells to clear a circulating pathogen infection[29]. Thus far, we have compared the effect of physiological D-lactate and L-lactate on single cell types *in vitro*. It is unknown how lactate may alter the communication between immune and metabolic cells like macrophages and hepatocytes. An important future direction is to co-culture or trans-well culture primary mouse hepatocytes and macrophages. One important goal would be to identify if and how macrophages can relay inflammatory signals to alter metabolism in hepatocytes, including measurement of changes in D-lactate and L-lactate metabolism, glucose production and lipogenesis. These results are important for understanding how D-lactate could contribute to aspects of type 2 diabetes and NAFLD.

5.5 Limitations

There are several limitations to this thesis. Cell viability in HEK-293T, RAW 264.7, BMDMs and primary hepatocytes in response to increasing doses of

lactate was not quantitatively determined. The effect of high doses of D-lactate and L-lactate on cell viability, especially in HEK-293T cells where a lactate dose-response of 1 μM-10 mM was performed, should be determined to ensure that the observed inflammatory responses were not caused by impaired cell viability. Another key consideration is whether 5 mM-10 mM D-lactate or L-lactate alters treatment media pH, which may also cause impaired cellular and immune function.

After initial experiments, it was identified that differentiating BMDMs with recombinant GM-CSF and M-CSF and co-stimulating with IFN-y revealed that D-lactate was more inflammatory than L-lactate in these macrophages exposed to microbial components. Experiments performed in RAW 264.7 cells or HEK-293T cells were not co-stimulated with IFN-y and may not respond to lactate comparably to activated macrophages. Therefore, these cell models were used for initial investigative purposes before translating the lactate treatments into primary macrophages. We also did not solve if differentiation with recombinant GM-CSF and M-CSF or co-stimulation with IFN-y (or both) was the factor in programming macrophages to respond to D-lactate differently than L-lactate.

The effect of chemical lactate inhibitors on NO production was unexpected. αCHC is a known antagonist of MCT-1 and has been used extensively in the literature, but it may have non-specific effects on NO. Although 3-OBA has been widely used by others as a GPR81 inhibitor, it has not been confirmed as an antagonist of GPR81. This is a major limitation in interpreting the

data and determining the efficacy of αCHC and 3-OBA as reliable lactate transporter inhibitors.

6.0 CONCLUSION

The role of D-lactate in metabolic inflammation was not well investigated in previous research. This was a key knowledge gap since L-lactate and D-lactate are rarely (if ever) included in the media during immune cell assessments and previous tests have not been done comparing physiological doses of L- versus D-lactate. Here, we have optimized an *in vitro* model to test the effect of physiological D-lactate and L-lactate in macrophages to understand how these lactate enantiomers influence inflammation. L- or D-lactate alone does not alter immunity. Hence, our model included combinations of low-level bacterial components that are ligands for pattern recognition receptors and physiological doses of L- and/or D-lactate. We showed that D-lactate promotes higher inflammation than L-lactate in macrophages evidenced by higher levels of the inflammatory cytokine IL-6, higher NO production and higher NLRP3 inflammasome activation after exposure to bacterial cell wall components. Higher levels of microbial-derived D-lactate may polarize macrophages toward NO production and activate the NLRP3 inflammasome in the liver. An important future direction is to investigate the role of lactate in the immune-metabolic relationship between macrophages and hepatocytes. Our research may lead to investigating whether the effect of D-lactate on inflammation *in vitro* occurs *in* vivo and participates in altering metabolic disease processes. Identifying the role of microbial D-lactate in metabolic disease may lead to the development of interventions that lower D-lactate and lower risk factors for T2D and NAFLD.

7.0 REFERENCES

1. Twells, L. K., Gregory, D. M., Reddigan, J. & Midodzi, W. K. Current and predicted prevalence of obesity in Canada: a trend analysis. *C. Open* **2**, E18–E26 (2014).
2. Tran, B. X., Nair, A. V., Kuhle, S., Ohinmaa, A. & Veugelers, P. J. Cost analyses of obesity in Canada: Scope, quality, and implications. *Cost Effectiveness and Resource Allocation* vol. 11 (2013).
3. Anis, A. H. *et al.* Obesity and overweight in Canada: an updated cost-of-illness study. *Obes. Rev.* **11**, 31–40 (2010).
4. Obesity in Canada - Obesity Canada. https://obesitycanada.ca/obesity-in-canada/.
5. Guh, D. P. *et al.* The incidence of co-morbidities related to obesity and overweight: A systematic review and meta-analysis. *BMC Public Health* **9**, 1–20 (2009).
6. Worldwide trends in diabetes since 1980: a pooled analysis of 751 population-based studies with 4.4 million participants. *Lancet (London, England)* **387**, 1513–1530 (2016).
7. Lean, M. E. J. *et al.* Durability of a primary care-led weight-management intervention for remission of type 2 diabetes: 2-year results of the DiRECT open-label, cluster-randomised trial. *Lancet Diabetes Endocrinol.* **7**, 344–355 (2019).
8. Shively, C. A. *et al.* Mediterranean versus Western Diet Effects on Caloric Intake, Obesity, Metabolism, and Hepatosteatosis in Nonhuman Primates. *Obesity* **27**, 777–784 (2019).
9. Parrott, J. *et al.* American Society for Metabolic and Bariatric Surgery Integrated Health Nutritional Guidelines for the Surgical Weight Loss Patient 2016 Update: Micronutrients. *Surg. Obes. Relat. Dis.* **13**, 727–741 (2017).
10. Madsen, L. R., Baggesen, L. M., Richelsen, B. & Thomsen, R. W. Effect of

Roux-en-Y gastric bypass surgery on diabetes remission and complications in individuals with type 2 diabetes: a Danish population-based matched cohort study. *Diabetologia* **62**, 611–620 (2019).

11. Kusminski, C. M., Bickel, P. E. & Scherer, P. E. Targeting adipose tissue in the treatment of obesity-associated diabetes. *Nature Reviews Drug Discovery* vol. 15 639–660 (2016).
12. Jung, U. J. & Choi, M. S. Obesity and Its Metabolic Complications: The Role of Adipokines and the Relationship between Obesity, Inflammation, Insulin Resistance, Dyslipidemia and Nonalcoholic Fatty Liver Disease. *Int. J. Mol. Sci. 2014, Vol. 15, Pages 6184-6223* **15**, 6184–6223 (2014).
13. Lolmède, K., Duffaut, C., Zakaroff-Girard, A. & Bouloumié, A. Immune cells in adipose tissue: Key players in metabolic disorders. *Diabetes Metab.* **37**, 283–290 (2011).
14. Bertola, A. *et al.* Identification of adipose tissue dendritic cells correlated with obesity-associated insulin-resistance and inducing Th17 responses in mice and patients. *Diabetes* **61**, 2238–2247 (2012).
15. Sun, S., Ji, Y., Kersten, S. & Qi, L. Mechanisms of inflammatory responses in obese adipose tissue. *Annu. Rev. Nutr.* **32**, 261–286 (2012).
16. Sun, B. & Karin, M. Obesity, inflammation, and liver cancer. *J. Hepatol.* **56**, 704–713 (2012).
17. Jarrar, M. H. *et al.* Adipokines and cytokines in non-alcoholic fatty liver disease. *Aliment. Pharmacol. Ther.* **27**, 412–421 (2008).
18. Mogensen, T. H. Pathogen recognition and inflammatory signaling in innate immune defenses. *Clin. Microbiol. Rev.* **22**, 240–273 (2009).
19. Girardin, S. E. *et al.* Nod1 detects a unique muropeptide from gram-negative bacterial peptidoglycan. *Science (80-.).* **300**, 1584–1587 (2003).
20. Kawasaki, T. & Kawai, T. Toll-like receptor signaling pathways. *Frontiers in Immunology* vol. 5 461 (2014).
21. Ahmad, R. *et al.* Elevated expression of the toll like receptors 2 and 4 in

obese individuals: its significance for obesity-induced inflammation. *J. Inflamm. (Lond).* **9**, 48 (2012).

22. Könner, A. C. & Brüning, J. C. Toll-like receptors: linking inflammation to metabolism. *Trends Endocrinol. Metab.* **22**, 16–23 (2011).
23. Cani, P. D. *et al.* Changes in gut microbiota control metabolic endotoxemia-induced inflammation in high-fat diet-induced obesity and diabetes in mice. *Diabetes* **57**, 1470–1481 (2008).
24. Cani, P. D. *et al.* Metabolic endotoxemia initiates obesity and insulin resistance. *Diabetes* **56**, 1761–1772 (2007).
25. Todoric, J. *et al.* Fructose stimulated de novo lipogenesis is promoted by inflammation. *Nat. Metab.* **2**, 1034–1045 (2020).
26. Schroeder, B. O. & Bäckhed, F. Signals from the gut microbiota to distant organs in physiology and disease. *Nature Medicine* vol. 22 1079–1089 (2016).
27. Million, M. *et al.* Obesity-associated gut microbiota is enriched in Lactobacillus reuteri and depleted in Bifidobacterium animalis and Methanobrevibacter smithii. *Int. J. Obes. (Lond).* **36**, 817 (2012).
28. Wang, Y. *et al.* Phocea, Pseudoflavonifractor and Lactobacillus intestinalis: Three Potential Biomarkers of Gut Microbiota That Affect Progression and Complications of Obesity-Induced Type 2 Diabetes Mellitus. *Diabetes, Metab. Syndr. Obes. Targets Ther.* **13**, 835 (2020).
29. McDonald, B. *et al.* Programing of an Intravascular Immune Firewall by the Gut Microbiota Protects against Pathogen Dissemination during Infection. *Cell Host Microbe* **28**, 660-668.e4 (2020).
30. Tremaroli, V. & Backhed, F. Functional interactions between the gut microbiota and host metabolism. *Nature* **489**, 242–249 (2012).
31. Bouter, K. E., van Raalte, D. H., Groen, A. K. & Nieuwdorp, M. Role of the Gut Microbiome in the Pathogenesis of Obesity and Obesity-Related Metabolic Dysfunction. *Gastroenterology* **152**, 1671–1678 (2017).

32. Ridaura, V. K. *et al.* Gut microbiota from twins discordant for obesity modulate metabolism in mice. *Science (80-.).* **341**, (2013).
33. Bäckhed, F. *et al.* The gut microbiota as an environmental factor that regulates fat storage. *Proc. Natl. Acad. Sci. U. S. A.* **101**, 15718–15723 (2004).
34. Turnbaugh, P. J. *et al.* An obesity-associated gut microbiome with increased capacity for energy harvest. *Nat. 2006 4447122* **444**, 1027–1031 (2006).
35. Peters, B. A. *et al.* A taxonomic signature of obesity in a large study of American adults OPEN. doi:10.1038/s41598-018-28126-1.
36. Utzschneider, K. M., Kratz, M., Damman, C. J. & Hullarg, M. Mechanisms Linking the Gut Microbiome and Glucose Metabolism. *J. Clin. Endocrinol. Metab.* **101**, 1445 (2016).
37. Ley, R. E. *et al.* Obesity alters gut microbial ecology. *Proc. Natl. Acad. Sci. U. S. A.* **102**, 11070–11075 (2005).
38. Ley, R. E., Turnbaugh, P. J., Klein, S. & Gordon, J. I. Microbial ecology: Human gut microbes associated with obesity. *Nature* **444**, 1022–1023 (2006).
39. Foley, K. P. *et al.* Gut microbiota impairs insulin clearance in obese mice. *Mol. Metab.* **42**, (2020).
40. Membrez, M. *et al.* Gut microbiota modulation with norfloxacin and ampicillin enhances glucose tolerance in mice. *FASEB J.* **22**, 2416–2426 (2008).
41. Jastroch, M., Ussar, S. & Keipert, S. Gut Microbes Controlling Blood Sugar: No Fire Required! *Cell Metab.* **31**, 443–444 (2020).
42. Krisko, T. I. *et al.* Dissociation of Adaptive Thermogenesis from Glucose Homeostasis in Microbiome-Deficient Mice. *Cell Metab.* **31**, 592-604.e9 (2020).
43. Caesar, R., Tremaroli, V., Kovatcheva-Datchary, P., Cani, P. D. &

Bäckhed, F. Crosstalk between gut microbiota and dietary lipids aggravates WAT inflammation through TLR signaling. *Cell Metab.* **22**, 658–668 (2015).

44. Scott, M. J., Chen, C., Sun, Q. & Billiar, T. R. Hepatocytes express functional NOD1 and NOD2 receptors: A role for NOD1 in hepatocyte CC and CXC chemokine production. (2010) doi:10.1016/j.jhep.2010.04.026.
45. Mazewski, C., Perez, R. E., Fish, E. N. & Platanias, L. C. Type I Interferon (IFN)-Regulated Activation of Canonical and Non-Canonical Signaling Pathways. *Front. Immunol.* **11**, 3025 (2020).
46. Schertzer, J. D. *et al.* NOD1 Activators Link Innate Immunity to Insulin Resistance. *Diabetes* **60**, 2206–2215 (2011).
47. Cori, C. F. & Cori, G. T. Glycogen formation in the liver from D- and L-lactic acid. *J. Biol. Chem.* **81**, 389–403 (1929).
48. Farhana, A. & Lappin, S. L. *Biochemistry, Lactate Dehydrogenase (LDH)*. *StatPearls* (StatPearls Publishing, 2020).
49. Ewaschuk, J. B., Naylor, J. M. & Zello, G. A. D-Lactate in Human and Ruminant Metabolism. *J. Nutr.* **135**, 1619–1625 (2005).
50. de Bari, L., Atlante, A., Guaragnella, N., Principato, G. & Passarella, S. D-Lactate transport and metabolism in rat liver mitochondria. *Biochem. J.* **365**, 391–403 (2002).
51. Flick, M. J. & Konieczny, S. F. Identification of putative mammalian d-lactate dehydrogenase enzymes. *Biochem. Biophys. Res. Commun.* **295**, 910–916 (2002).
52. Brooks, G. A. The Science and Translation of Lactate Shuttle Theory. *Cell Metab.* **27**, 757–785 (2018).
53. Ratliff, D. M., Vander Jagt, D. J., Eaton, R. P. & Vander Jagt, D. L. Increased levels of methylglyoxal-metabolizing enzymes in mononuclear and polymorphonuclear cells from insulin-dependent diabetic patients with diabetic complications: aldose reductase, glyoxalase I, and glyoxalase II--a

clinical research center study. *J. Clin. Endocrinol. Metab.* **81**, 488–492 (1996).

54. Chen, C. N. (Joyce) *et al.* Diet-induced obesity accelerates blood lactate accumulation of rats in response to incremental exercise to maximum. *Am. J. Physiol. - Regul. Integr. Comp. Physiol.* **313**, R601–R607 (2017).
55. Datta, S. & Chakrabarti, N. Age related rise in lactate and its correlation with lactate dehydrogenase (LDH) status in post-mitochondrial fractions isolated from different regions of brain in mice. *Neurochem. Int.* **118**, 23–33 (2018).
56. Murray, M. J., Gonze, M. D., Nowak, L. R. & Cobb, C. F. Serum D(-)-lactate levels as an aid to diagnosing acute intestinal ischemia. *Am. J. Surg.* **167**, 575–578 (1994).
57. Song, W. B. *et al.* Soluble intercellular adhesion molecule-1, D-lactate and diamine oxidase in patients with inflammatory bowel disease. *World J. Gastroenterol.* **15**, 3916–3919 (2009).
58. Talasniemi, J. P., Pennanen, S., Savolainen, H., Niskanen, L. & Liesivuori, J. Analytical investigation: Assay of d-lactate in diabetic plasma and urine. *Clin. Biochem.* **41**, 1099–1103 (2008).
59. Scheijen, J. L. J. M. *et al.* L(+) and D(−) Lactate Are Increased in Plasma and Urine Samples of Type 2 Diabetes as Measured by a Simultaneous Quantification of L(+) and D(−) Lactate by Reversed-Phase Liquid Chromatography Tandem Mass Spectrometry. *Exp. Diabetes Res.* **2012**, (2012).
60. Rodríguez-Mortera, R. *et al.* Higher D-lactate levels are associated with higher prevalence of small dense low-density lipoprotein in obese adolescents. *Clin. Chem. Lab. Med.* **56**, 1100–1108 (2018).
61. Ross, J. M. *et al.* High brain lactate is a hallmark of aging and caused by a shift in the lactate dehydrogenase A/B ratio. doi:10.1073/pnas.1008189107.

62. Thorburn, A. N., Macia, L. & Mackay, C. R. Diet, metabolites, and 'western-lifestyle' inflammatory diseases. *Immunity* **40**, 833–842 (2014).
63. Blad, C. C., Tang, C. & Offermanns, S. G protein-coupled receptors for energy metabolites as new therapeutic targets. *Nat. Rev. Drug Discov. 2012 118* **11**, 603–619 (2012).
64. Hasegawa, H. *et al.* Determination of serum d-lactic and l-lactic acids in normal subjects and diabetic patients by column-switching HPLC with pre-column fluorescence derivatization. *Anal. Bioanal. Chem.* **377**, 886–891 (2003).
65. Song, Y. *et al.* Inhibition of lactate dehydrogenase A suppresses inflammatory response in RAW 264.7 macrophages. *Mol. Med. Rep.* **19**, 629–637 (2019).
66. Gottfried, E. *et al.* Tumor-derived lactic acid modulates dendritic cell activation and antigen expression. *Blood* **107**, 2013–2021 (2006).
67. Colegio, O. R. *et al.* Functional polarization of tumour-associated macrophages by tumour-derived lactic acid. *Nature* **513**, 559–563 (2014).
68. Fischer, K. *et al.* Inhibitory effect of tumor cell-derived lactic acid on human T cells. *Blood* **109**, 3812–3819 (2007).
69. Hoque, R., Farooq, A., Ghani, A., Gorelick, F. & Mehal, W. Z. Lactate reduces liver and pancreatic injury in toll-like receptor- and inflammasome-mediated inflammation via gpr81-mediated suppression of innate immunity. *Gastroenterology* **146**, 1763–1774 (2014).
70. Errea, A. *et al.* Lactate Inhibits the Pro-Inflammatory Response and Metabolic Reprogramming in Murine Macrophages in a GPR81-Independent Manner. *PLoS One* **11**, e0163694 (2016).
71. Pucino, V. *et al.* Lactate Buildup at the Site of Chronic Inflammation Promotes Disease by Inducing CD4+ T Cell Metabolic Rewiring. *Cell Metab.* **30**, 1055-1074.e8 (2019).
72. Huynh, V., D'Angelo, A. D. & Wylie, R. G. Tunable degradation of low-

fouling carboxybetaine-hyaluronic acid hydrogels for applications in cell encapsulation. *Biomed. Mater.* **14**, 55003 (2019).

73. Liebergall, S. R. *et al.* Inflammation triggers liver X receptor -dependent lipogenesis. *Mol. Cell. Biol* (2019) doi:10.1128/MCB.00364-19.
74. Oishi, Y. *et al.* SREBP1 Contributes to Resolution of Pro-inflammatory TLR4 Signaling by Reprogramming Fatty Acid Metabolism. *Cell Metab.* **25**, 412–427 (2017).
75. Tilg, H. & Moschen, A. R. Evolution of Inflammation in Nonalcoholic Fatty Liver Disease: The Multiple Parallel Hits Hypothesis. (2010) doi:10.1002/hep.24001.
76. Zhao, L. *et al.* Chronic inflammation aggravates metabolic disorders of hepatic fatty acids in high-fat diet-induced obese mice. *Sci. Rep.* **5**, 1–12 (2015).
77. Li, Z. *et al.* Probiotics and antibodies to TNF inhibit inflammatory activity and improve nonalcoholic fatty liver disease. *Hepatology* **37**, 343–350 (2003).
78. Clementi, A. H., Gaudy, A. M., van Rooijen, N., Pierce, R. H. & Mooney, R. A. Loss of Kupffer cells in diet-induced obesity is associated with increased hepatic steatosis, STAT3 signaling, and further decreases in insulin signaling. *Biochim. Biophys. Acta - Mol. Basis Dis.* **1792**, 1062–1072 (2009).
79. Obstfeld, A. E. *et al.* C-C Chemokine Receptor 2 (CCR2) regulates the hepatic recruitment of myeloid cells that promote obesity-induced hepatic steatosis. *Diabetes* **59**, 916–925 (2010).
80. Yang, K. *et al.* Lactate Suppresses Macrophage Pro-Inflammatory Response to LPS Stimulation by Inhibition of YAP and NF-κB Activation via GPR81-Mediated Signaling. *Front. Immunol.* **11**, 2610 (2020).
81. Bailey, J. D. *et al.* Isolation and culture of murine bone marrow-derived macrophages for nitric oxide and redox biology. *Nitric oxide Biol. Chem.*

100–**101**, 17–29 (2020).

82. Tayeh, M. A. & Marlettas, M. A. Macrophage Oxidation of L-Arginine to Nitric Oxide, Nitrite, and Nitrate. *J. Biol. Chem.* **264**, 19654–19658 (1989).
83. Mohammad Nezhady, M. A. & Chemtob, S. 3-OBA Is Not an Antagonist of GPR81. *Front. Pharmacol.* **12**, 3759 (2022).
84. Hui, S. *et al.* Glucose feeds the TCA cycle via circulating lactate. *Nature* **551**, 115–118 (2017).
85. Wang, L., He, H. W., Xing, Z. Q., Tang, B. & Zhou, X. Lactate induces alternative polarization (M2) of macrophages under lipopolysaccharide stimulation in vitro through G-protein coupled receptor 81. *Chin. Med. J. (Engl).* **133**, 1761–1763 (2020).
86. Mu, X. *et al.* Tumor-derived lactate induces M2 macrophage polarization via the activation of the ERK/STAT3 signaling pathway in breast cancer. *Cell Cycle* **17**, 428 (2018).
87. Orecchioni, M., Ghosheh, Y., Pramod, A. B. & Ley, K. Macrophage polarization: Different gene signatures in M1(Lps+) vs. Classically and M2(LPS-) vs. Alternatively activated macrophages. *Front. Immunol.* **10**, 1084 (2019).
88. Halestrap, A. P. & Wilson, M. C. Critical Review The Monocarboxylate Transporter Family-Role and Regulation. **64**, 109–119 (2012).
89. Hahn, E. L., Halestrap, A. P. & Gamelli, R. L. Expression of the lactate transporter MCT1 in macrophages. *Shock* **13**, 253–260 (2000).
90. Manning Fox, J. E., Meredith, D. & Halestrap, A. P. Characterisation of human monocarboxylate transporter 4 substantiates its role in lactic acid efflux from skeletal muscle. *J. Physiol.* **529 Pt 2**, 285–293 (2000).
91. Kong, L. *et al.* Monocarboxylate transporter 1 promotes classical microglial activation and pro-inflammatory effect via 6-phosphofructo-2-kinase/fructose-2, 6-biphosphatase 3. *J. Neuroinflammation* **16**, 1–12 (2019).

92. Manoharan, I., Prasad, P. D., Thangaraju, M. & Manicassamy, S. Lactate-Dependent Regulation of Immune Responses by Dendritic Cells and Macrophages. *Front. Immunol.* **12**, 3062 (2021).
93. Shen, Z. *et al.* Inhibition of G Protein-Coupled Receptor 81 (GPR81) Protects Against Ischemic Brain Injury. *CNS Neurosci. Ther.* **21**, 271–279 (2015).
94. Yang, K. *et al.* Lactate promotes macrophage HMGB1 lactylation, acetylation, and exosomal release in polymicrobial sepsis. *Cell Death Differ. 2021 291* **29**, 133–146 (2021).
95. Blad, C. C., Ahmed, K., IJzerman, A. P. & Offermanns, S. Biological and pharmacological roles of HCA receptors. *Adv. Pharmacol.* **62**, 219–250 (2011).
96. Lu, G. *et al.* Myeloid cell-derived inducible nitric oxide synthase suppresses M1 macrophage polarization. *Nat. Commun. 2015 61* **6**, 1–14 (2015).
97. Surewaard, B. G. J. *et al.* Identification and treatment of the Staphylococcus aureus reservoir in vivo. *J. Exp. Med.* **213**, 1141–1151 (2016).
98. Zhao, K., Huang, Z., Lu, H., Zhou, J. & Wei, T. Induction of inducible nitric oxide synthase increases the production of reactive oxygen species in RAW264.7 macrophages. *Biosci. Rep.* **30**, 233–241 (2010).
99. Harun-Or-Rashid, M. & Inman, D. M. Reduced AMPK activation and increased HCAR activation drive anti-inflammatory response and neuroprotection in glaucoma. *J. Neuroinflammation* **15**, 1–15 (2018).
100. Ridker, P. M. From CRP to IL-6 to IL-1: Moving Upstream To Identify Novel Targets for Atheroprotection. *Circ. Res.* **118**, 145 (2016).
101. Vandanmagsar, B. *et al.* The NLRP3 inflammasome instigates obesity-induced inflammation and insulin resistance. *Nat. Med.* **17**, 179–189 (2011).
102. Yao, Y., Xu, X. H. & Jin, L. Macrophage polarization in physiological and

pathological pregnancy. *Front. Immunol.* **10**, 792 (2019).

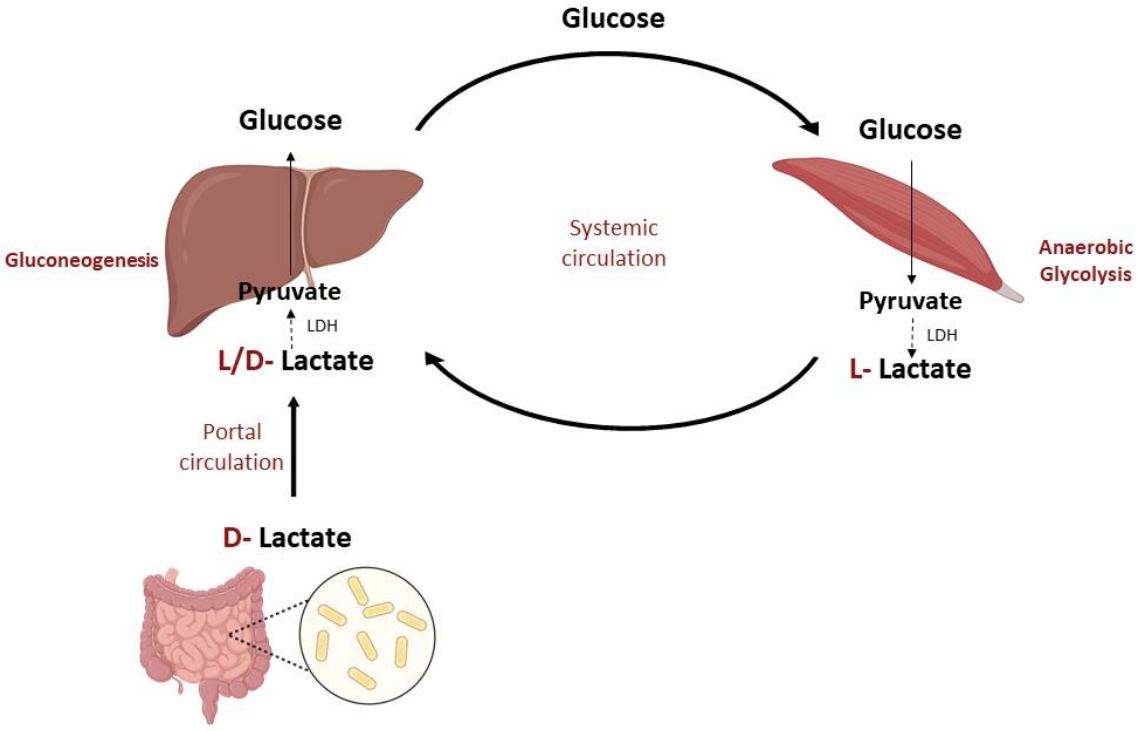

Figure 1: The Cori cycle.

Glucose is metabolized via anaerobic glycolysis into lactate, predominantly L-lactate. D-lactate is provided by gut microbiota via the portal circulation. Both L-lactate and D-lactate are used as substrates by the liver in host glucose synthesis such as gluconeogenesis.

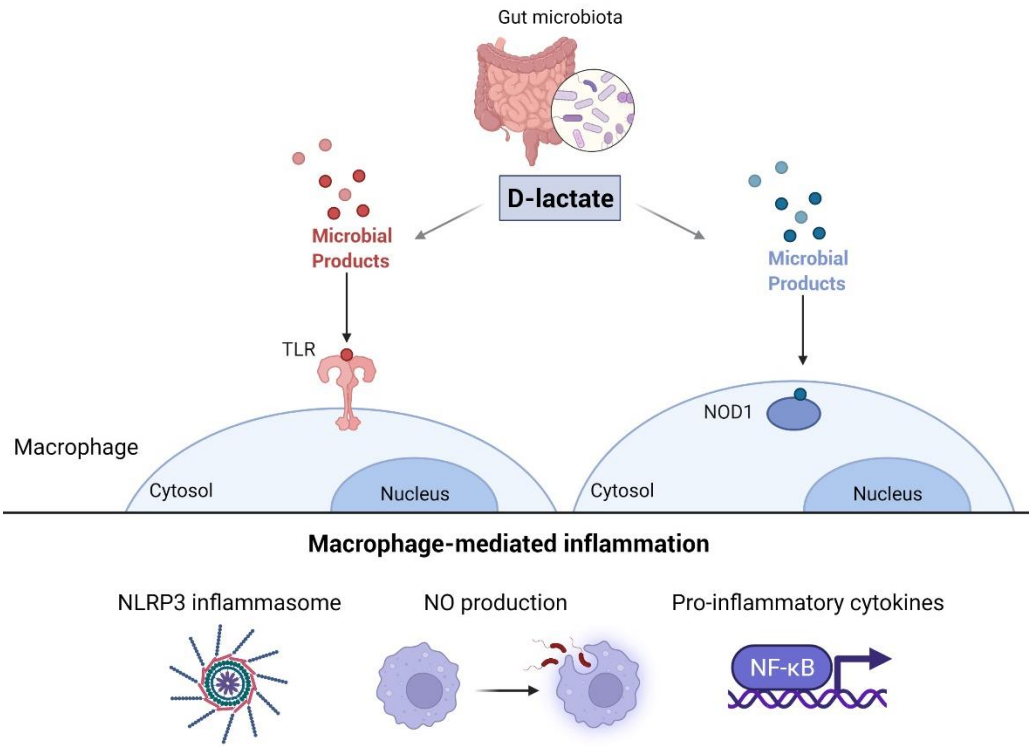

Figure 2: Immunogenic microbial products and metabolites can synergize to alter immune responses.

Non-immunogenic metabolites can synergize with microbial products from gut microbiota via PRR activation and modulate immune signalling.

A

	24 h		48 h	
	4°C	37°C	4°C	37°C
Vehicle	7.35	7.60	7.88	7.87
D-lactate (100 μM)	7.42	7.60	7.84	7.93
L-lactate (100 μM)	7.25	7.62	7.85	7.89
L-lactate (5 mM)	7.37	7.61	7.86	7.91
D-lactate (100 μM) + L-lactate (5 mM)	7.37	7.60	7.84	7.90

B

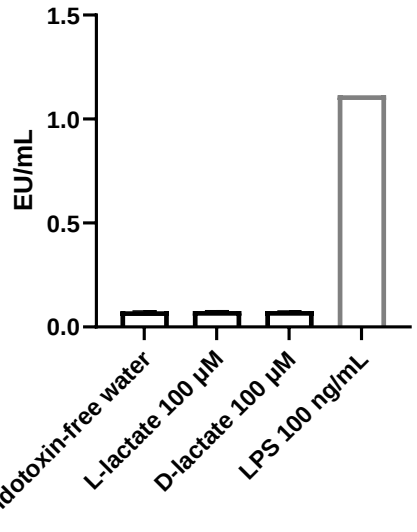

Figure 3: Endotoxin contamination and pH of lactate in media.

Measures of (**A**) pH and (**B**) endotoxin contamination levels in low-glucose DMEM with L-lactate and/or D-lactate. Values represented as mean ±SEM, n=1-3 for endotoxin contamination measurements.

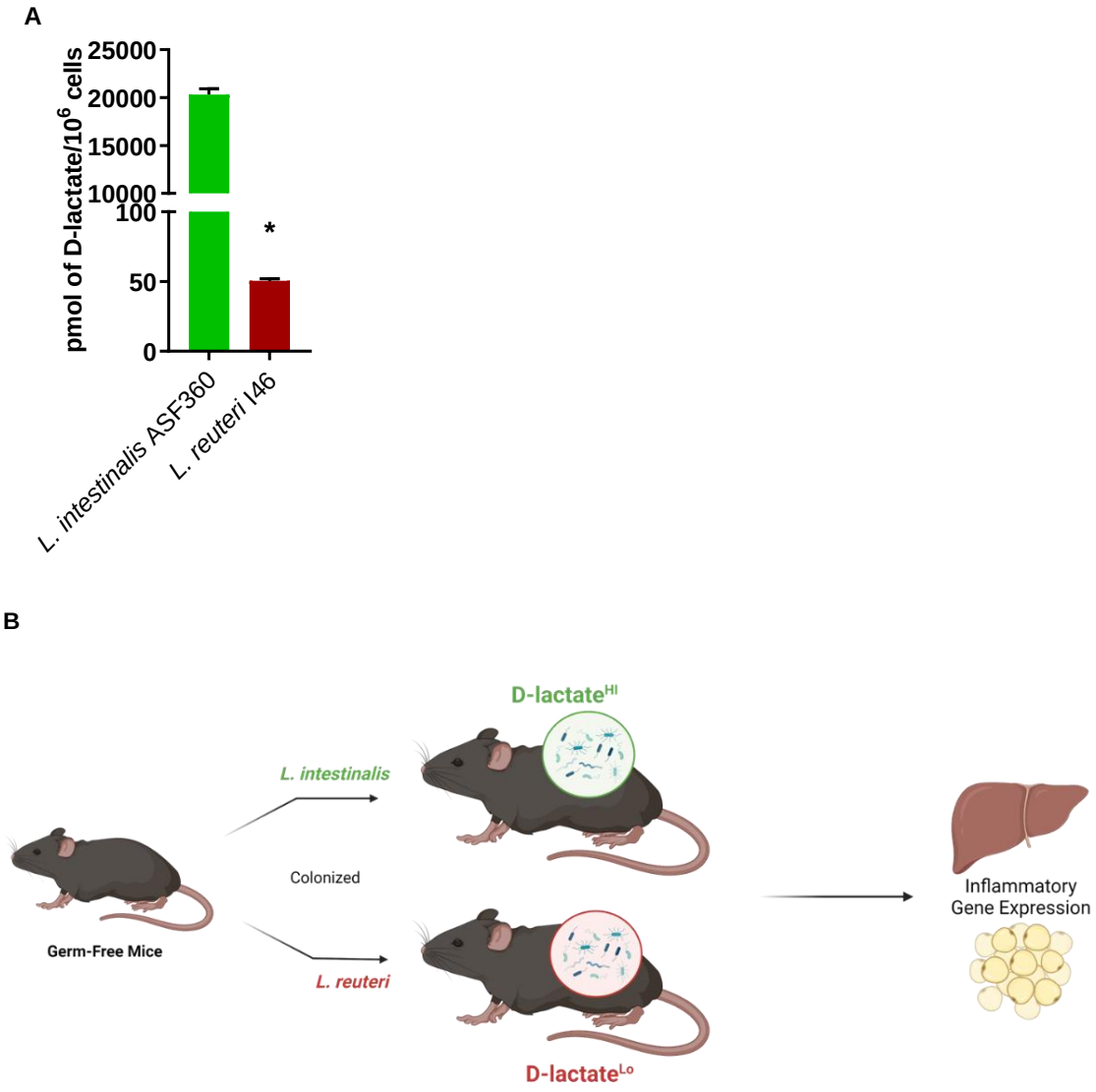

Figure 4: Schematic of experimental design and method of colonized GF mice.

Levels of D-lactate produced by *L. intestinalis* ASF360 and *L. reuteri* I46 were measured in pmol of D-lactate/10^6 cells by D-lactate colorimetric assay (**A**) and colonization of GF mice with high or low producers of D-lactate (**B**) performed by Dr. Anhê. Values are represented as mean ±SEM, n=3 for each group. *significantly different from *L. intestinalis* ASF360 by two-tailed parametric unpaired t-test.

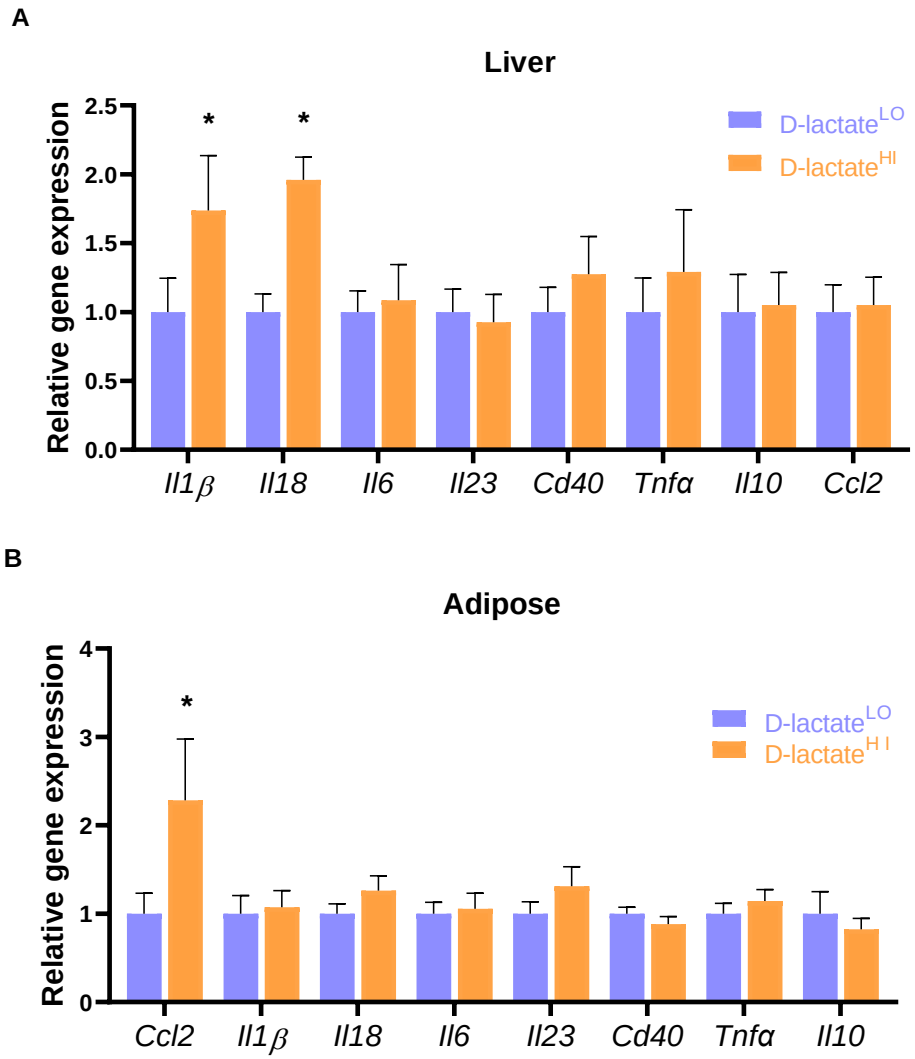

Figure 5: Inflammatory gene expression in GF mice colonized with high or low producers of D-lactate.

Relative gene expression in the liver (**A**) and adipose tissue (**B**) of mice colonized with *Lactobacillus reuteri* (D-lactate^{LO}) or *Lactobacillus intestinalis* (D-lactate^{HI}). Values are represented as mean ±SEM, n=10 for D-lactate^{HI} group and n=14 for D-lactate^{LO} group where each replicate represents a separate animal. Significant differences between D-lactate^{HI} and D-lactate^{LO} were found using two-tailed unpaired, nonparametric Mann-Whitney tests for non-normal data or two-tailed unpaired, parametric t-tests for normal data. *significantly different from the D-lactate^{LO} group.

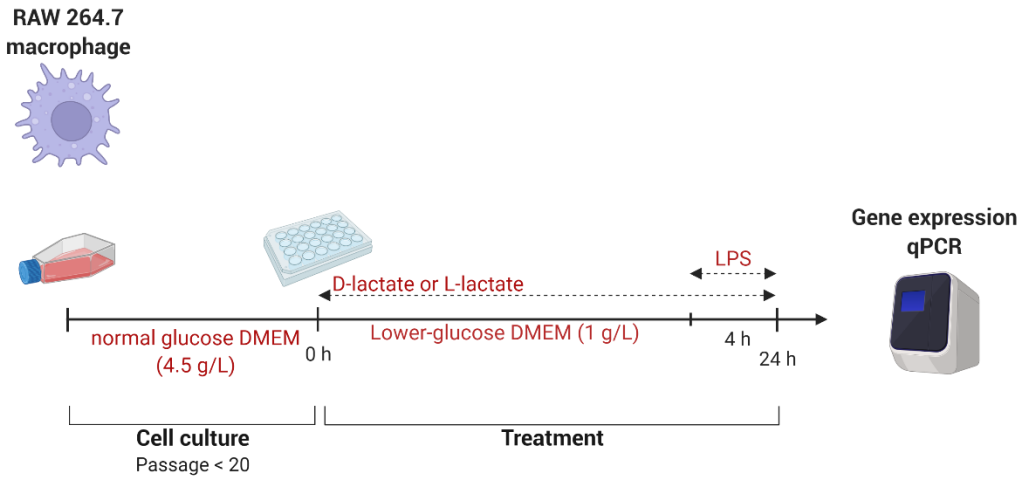

Figure 6: Schematic of RAW 264.7 macrophage experimental design and culture methods.

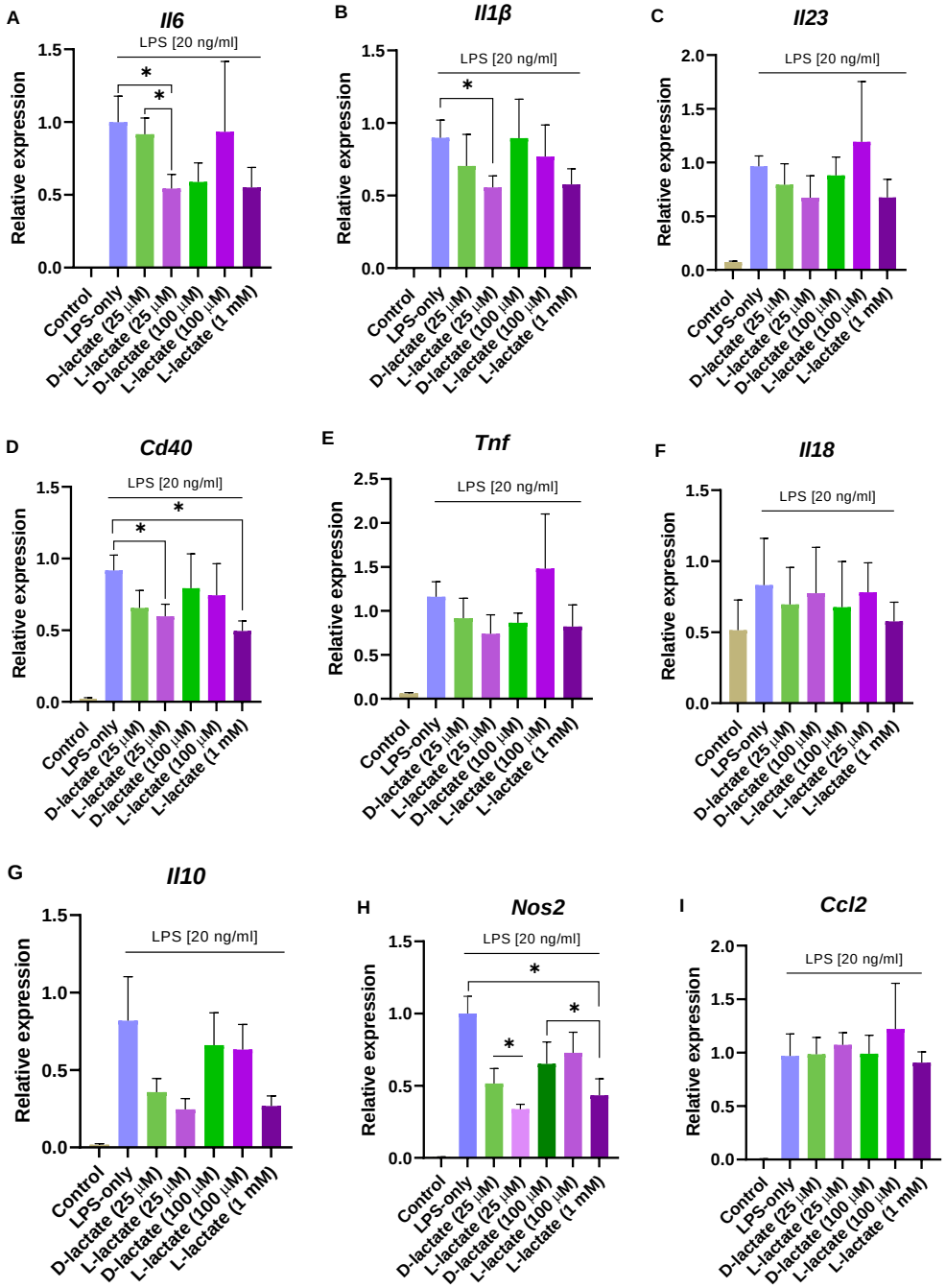
A
Il6
B
Il1β
C
Il23
D
Cd40
E
Tnf
F
Il18
G
Il10
H
Nos2
I
Ccl2
LPS [20 ng/ml]
Relative expression
Control
LPS-only
D-lactate (25 μM)
L-lactate (25 μM)
D-lactate (100 μM)
L-lactate (100 μM)
L-lactate (1 mM)

Figure 7: Inflammatory gene expression in RAW 264.7 macrophages during endotoxin exposure in response to physiological or equimolar lactate.

Changes in relative gene expression of (**A**) *Il6*, (**B**) *Il1β*, (**C**) *Il123*, (**D**) *Cd40,* (**E**) *Tnf*, (**F**) *Il18,* (**G**) *Il10,* (**H**) *Nos2* and (**I**) *Ccl2* in RAW 264.7 macrophages treated with D-lactate or L-lactate for 24 h and stimulated with LPS (20 ng/mL) for 4 h. Values represented as mean ±SEM, n=6 for all groups where each replicate represents a separate day or cell passage. Significant differences between D-lactate and L-lactate were found using a one-way ANOVA for normal data or Kruskal-Wallis test for non-normal data. *significantly different from the indicated group.

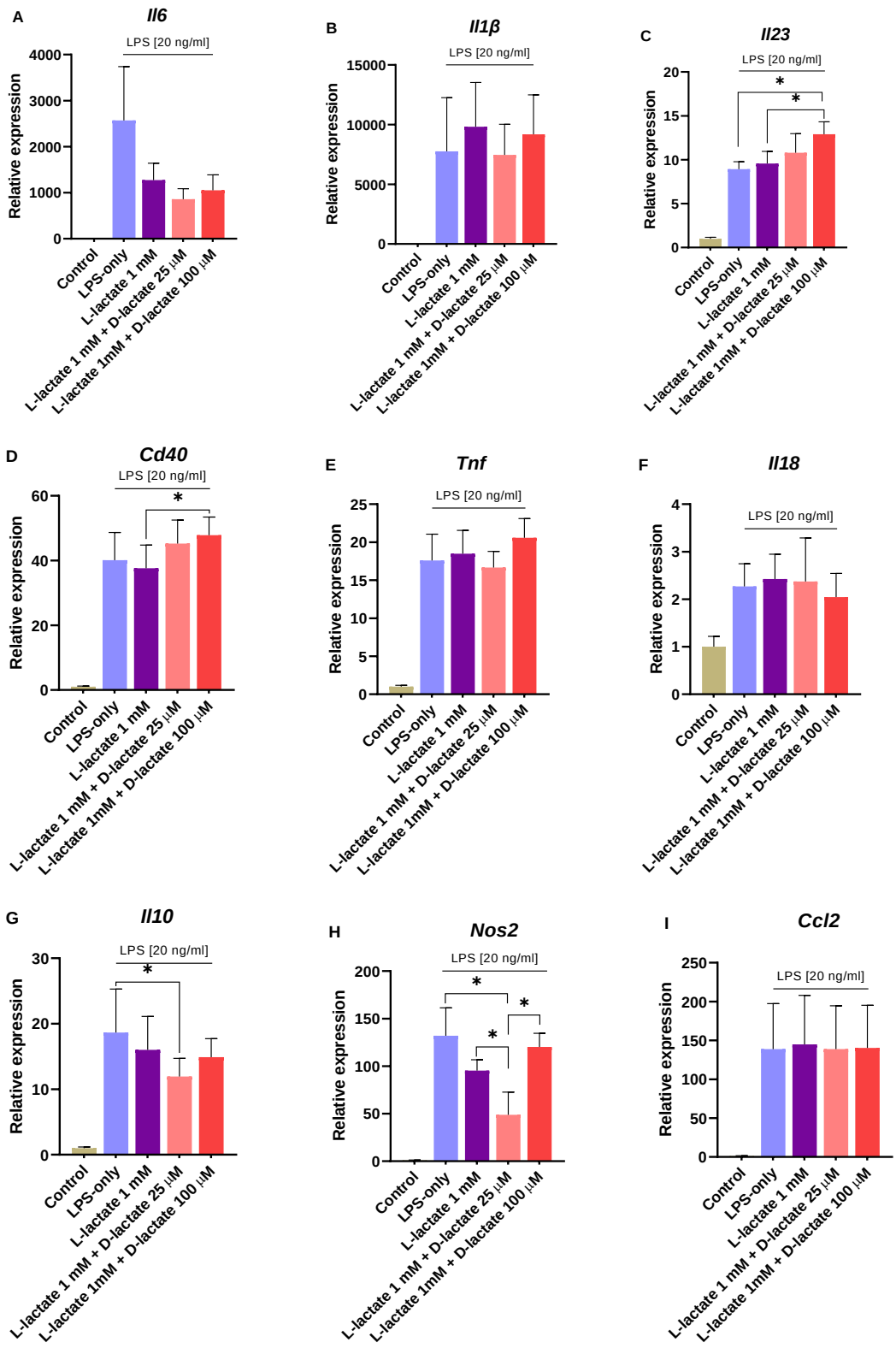
A
Il6
LPS [20 ng/ml]
Relative expression
4000
3000
2000
1000
0
B
Il1β
LPS [20 ng/ml]
Relative expression
15000
10000
5000
0
C
Il23
LPS [20 ng/ml]
*
*
Relative expression
20
15
10
5
0
D
Cd40
LPS [20 ng/ml]
*
Relative expression
60
40
20
0
E
Tnf
LPS [20 ng/ml]
Relative expression
25
20
15
10
5
0
F
Il18
LPS [20 ng/ml]
Relative expression
4
3
2
1
0
G
Il10
LPS [20 ng/ml]
*
Relative expression
30
20
10
0
H
Nos2
LPS [20 ng/ml]
*
*
*
Relative expression
200
150
100
50
0
I
Ccl2
LPS [20 ng/ml]
Relative expression
250
200
150
100
50
0
Control
LPS-only
L-lactate 1 mM
L-lactate 25 µM
L-lactate 1 mM + D-lactate 25 µM
L-lactate 1mM + D-lactate 100 µM

Figure 8: Inflammatory gene expression in RAW 264.7 macrophages during endotoxin exposure in response to D-lactate in the presence of L-lactate.

Changes in relative gene expression of (**A**) *Il6*, (**B**) *Il1β*, (**C**) *Il123*, (**D**) *Cd40,* (**E**) *Tnf*, (**F**) *Il18,* (**G**) *Il10,* (**H**) *Nos2* and (**I**) *Ccl2* in RAW 264.7 macrophages treated with D-lactate in the presence of L-lactate for 24h and stimulated with LPS (20 ng/mL) for 4h. Values represented as mean ±SEM, n=6 for all groups where each replicate (i.e., dot) represents a separate day or cell passage. Significant differences between groups were found using a one-way ANOVA for normal data or Kruskal-Wallis test for non-normal data. *significantly different from the indicated group

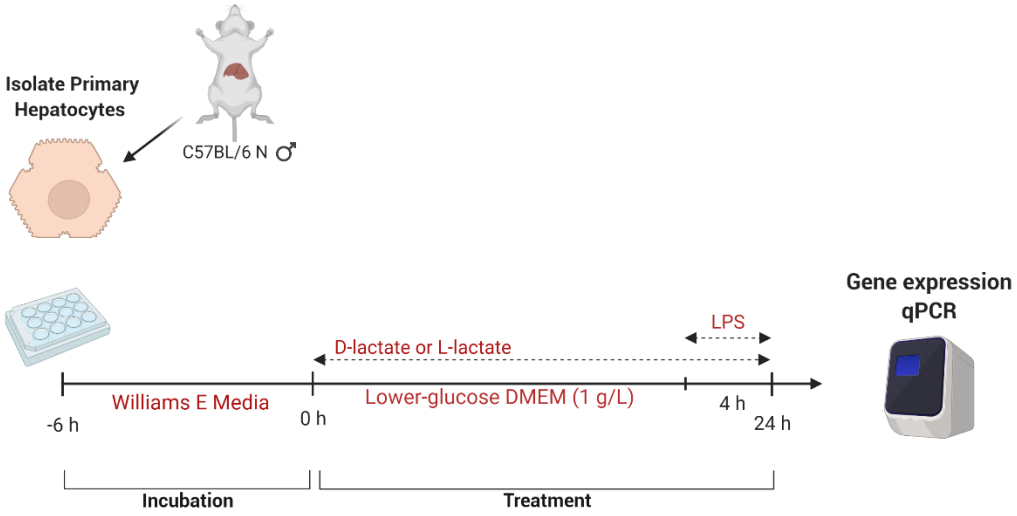

Figure 9: Schematic of experimental design and method of primary mouse hepatocyte culture.

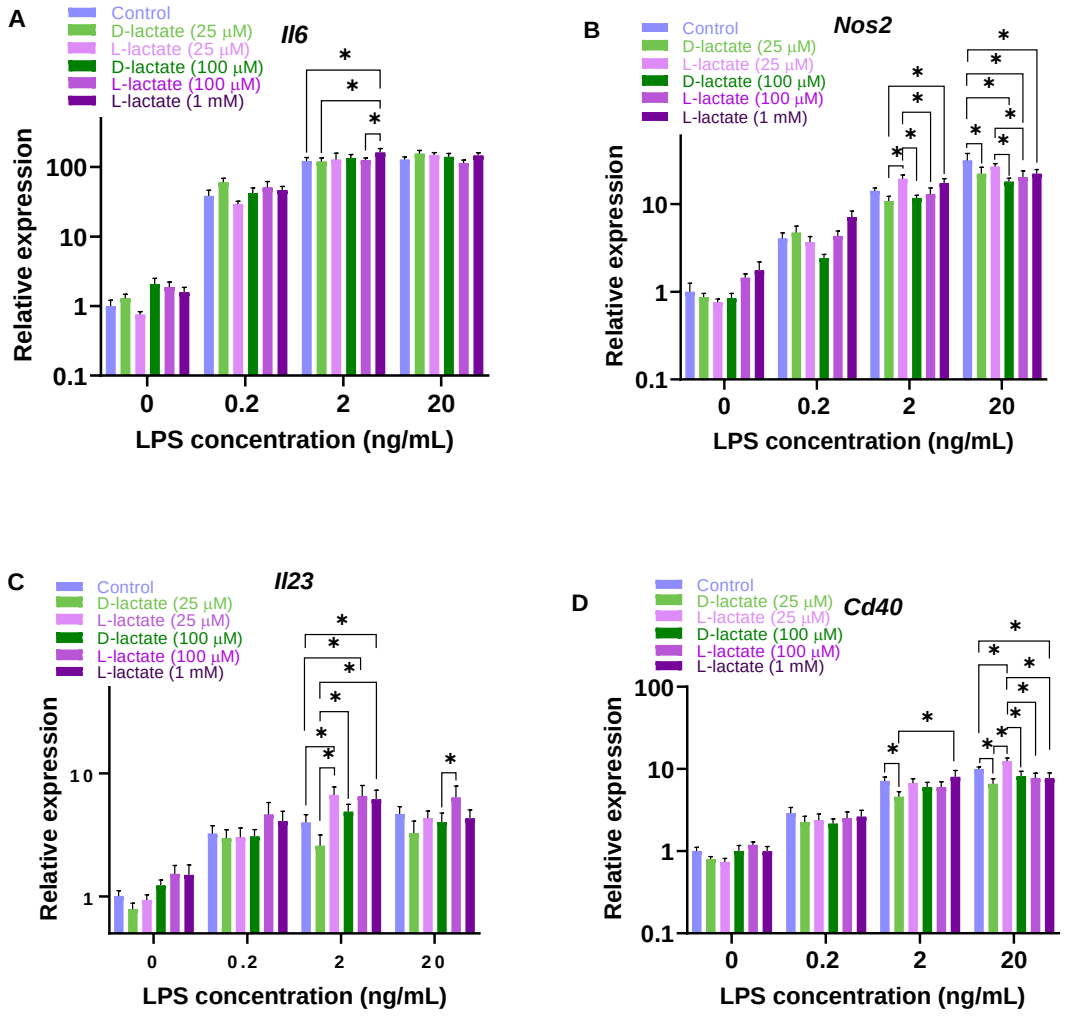

Figure 10: Inflammatory gene expression in primary mouse hepatocytes during endotoxin exposure in response to lactate.

Changes in relative gene expression in response to 0, 0.2, 2, 20 ng/mL LPS of (**A**) *Il6*, (**B**) *Nos2*, (**C**) *Il123* and (**D**) *Cd40* in primary mouse hepatocytes. Values are represented as mean ±SEM, n=9 for all groups where each replicate represents a separate day or animal. Significant differences between groups were found using the Fisher's LSD test. *significantly different from the indicated group by two-way ANOVA.

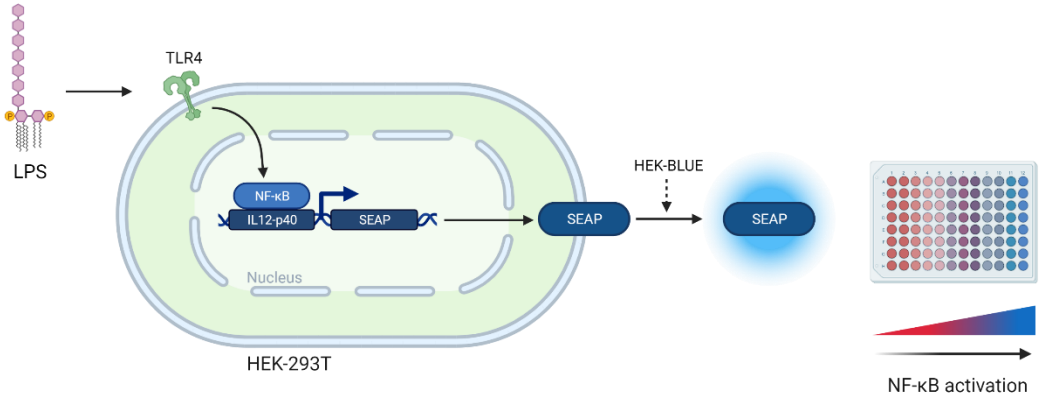

Figure 11: Schematic of NF-κB activation detection using HEK-293T TLR4 reporter cells.

Stimulation with a TLR4 ligand such as *E. coli* LPS activates NF-κB fused to an IL12-p40 promoter that regulates inducible SEAP production. Levels of SEAP secreted in the supernatant are proportional to NF-κB activation and measured using HEK-Blue™ Detection medium.

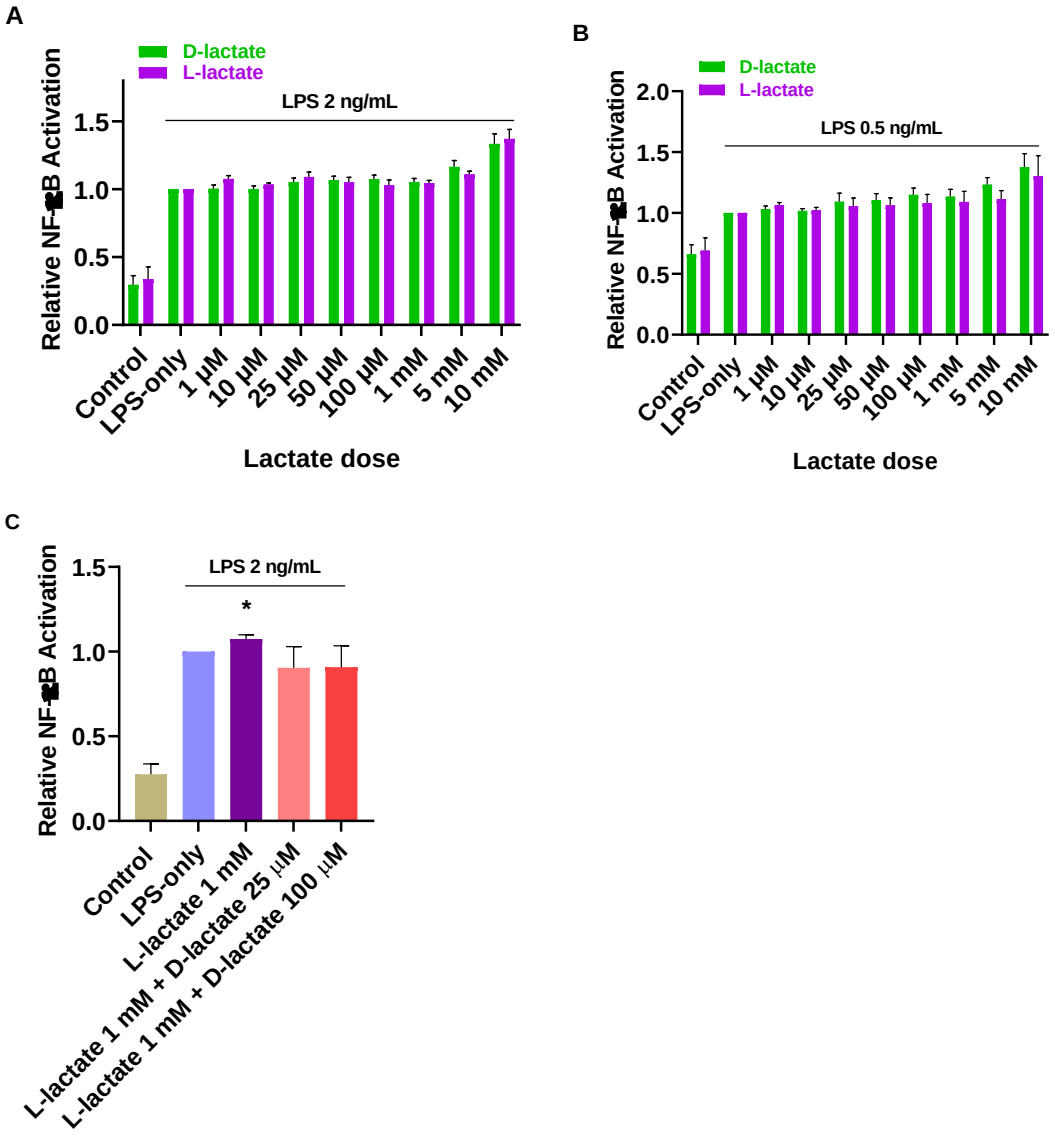

Figure 12: TLR4-mediated NF-κB activation during endotoxin exposure in response to D-lactate or L-lactate.

Relative NF-κB activation in response to (**A**) 1 µM-10 mM L-lactate or D-lactate during 2 ng/mL LPS exposure, (**B**) 1 µM-10 mM L-lactate or D-lactate during 0.5 ng/mL LPS exposure and (**C**) L-lactate 1 mM in the presence or absence of 25 µM or D-lactate 100 µM D-lactate during 2 ng/mL LPS exposure in HEK-293T TLR4 cells. Values represented as mean ±SEM, n=8 for all groups where each replicate represents a separate day or cell passage. Significant differences between groups were found using Kruskal-Wallis test for non-normal data. *significantly different from the indicated group.

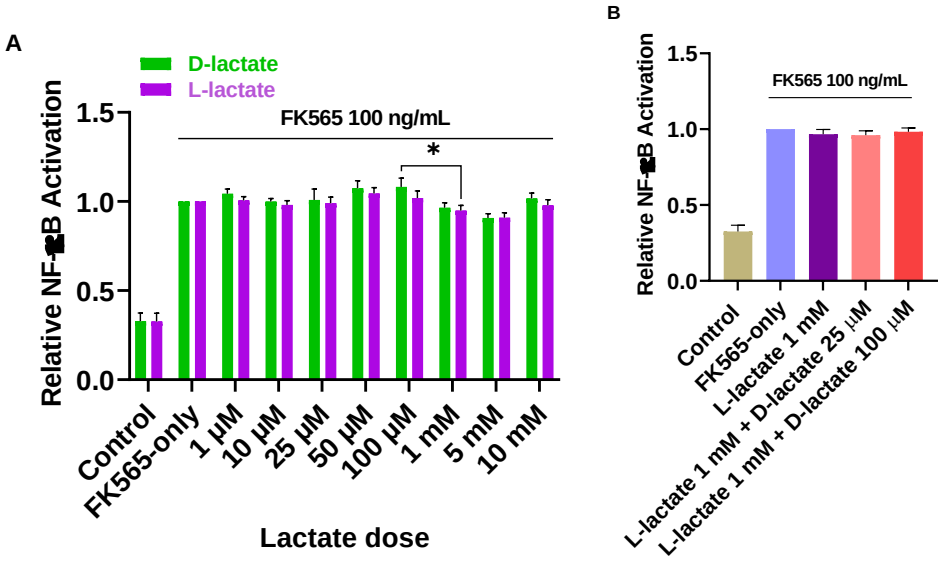

Figure 13: NOD1-mediated NF-κB activation during endotoxin exposure in response to lactate.

Relative NF-κB activation in response to (**A**)1 µM-10 mM L-lactate or D-lactate and (**B**) L-lactate 1 mM in the presence or absence of 25 µM or 100 µM D-lactate during NOD1 ligand 100 ng/mL FK565 exposure in HEK-293T NOD1 cells. Values represented as mean ±SEM, n=8-9 for all groups where each replicate represents a separate day or cell passage. Significant differences between 100 µM D-lactate and 1 mM L-lactate were found using the Fisher's LSD test for normal data. *significantly different by two-way ANOVA.

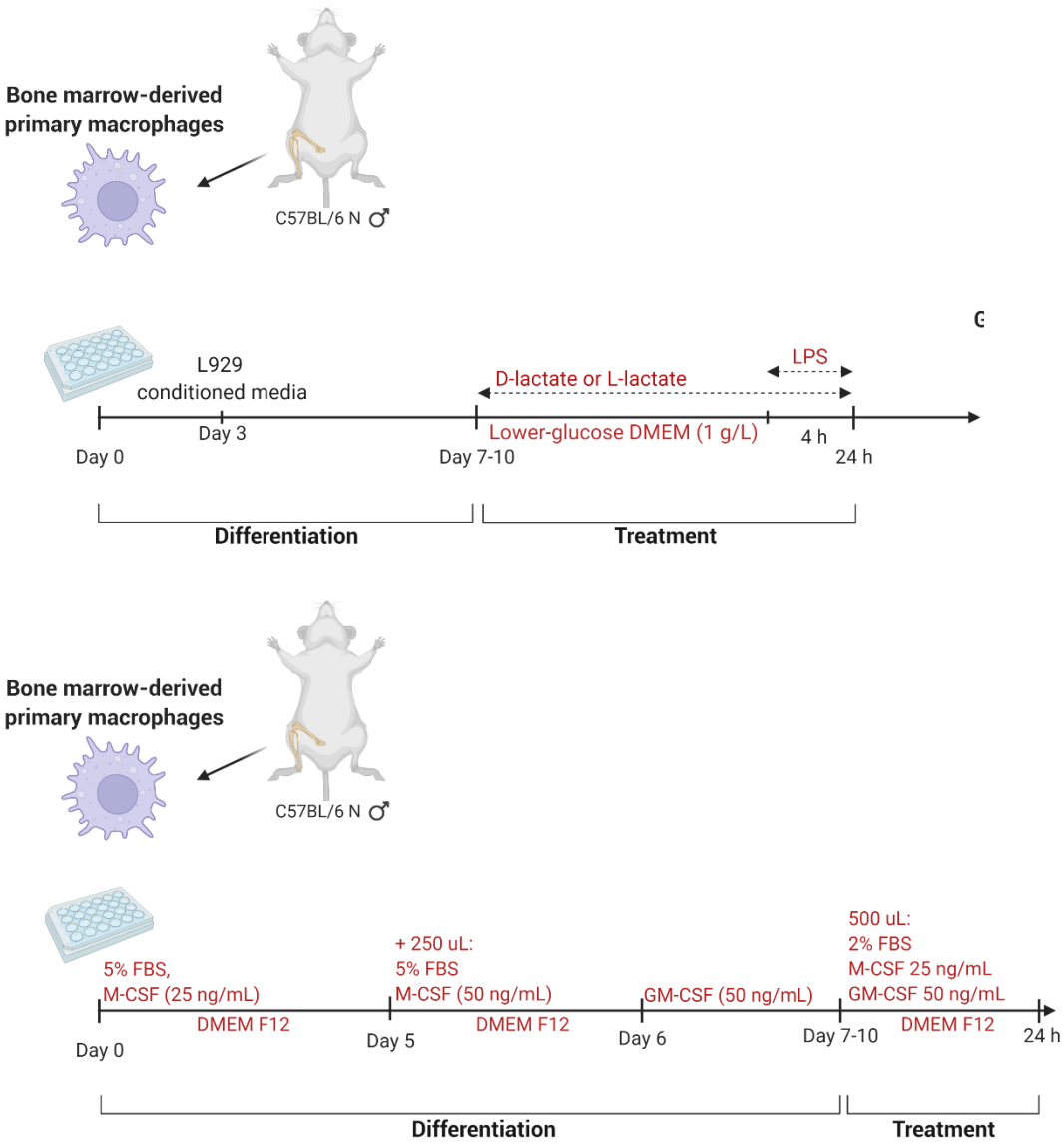

Figure 14: Schematic of bone marrow-derived macrophage experimental design and culture methods.

Methods of BMDM differentiation and cell culture using (**A**) L929 conditioned media or (**B**) recombinant macrophage colony-stimulating factors and IFN-γ co-stimulation adapted from Bailey *et al.*[81].

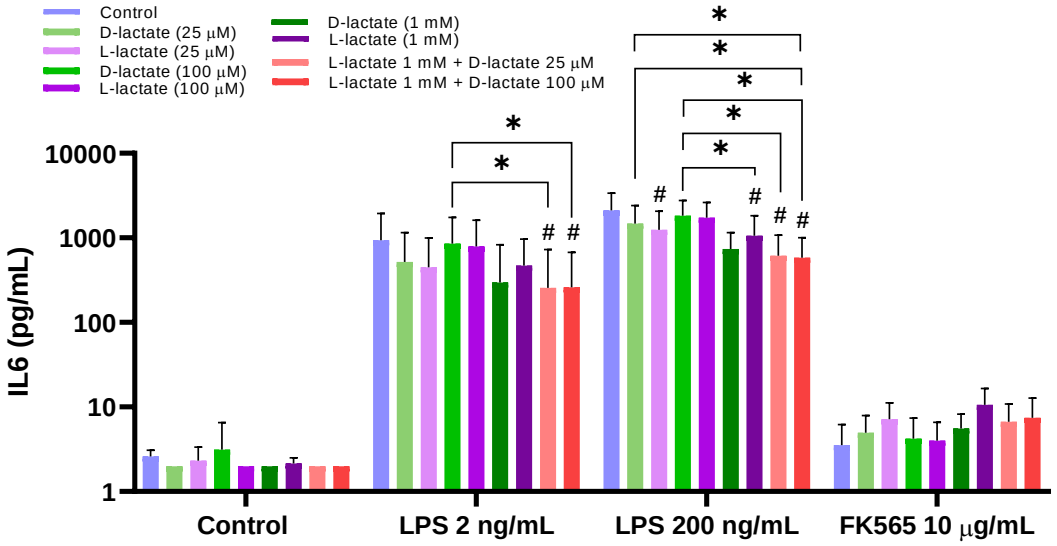

Figure 15: IL-6 release by BMDMs during endotoxin and muropeptide exposure in response to lactate.

IL-6 release in BMDMs treated with D-lactate, L-lactate or D-lactate in the presence of L-lactate for 48 h and stimulated with LPS (2 ng/mL), LPS (200 ng/mL) or FK565 (10 μg/mL) for 48 h. Values represented as mean ±SEM, n=9 for all groups where each replicate represents a separate day or animal. Significant differences between groups were found using Fisher's LSD test for normal data. *significantly different from the indicated group by two-way ANOVA. #significantly different from control by two-way ANOVA.

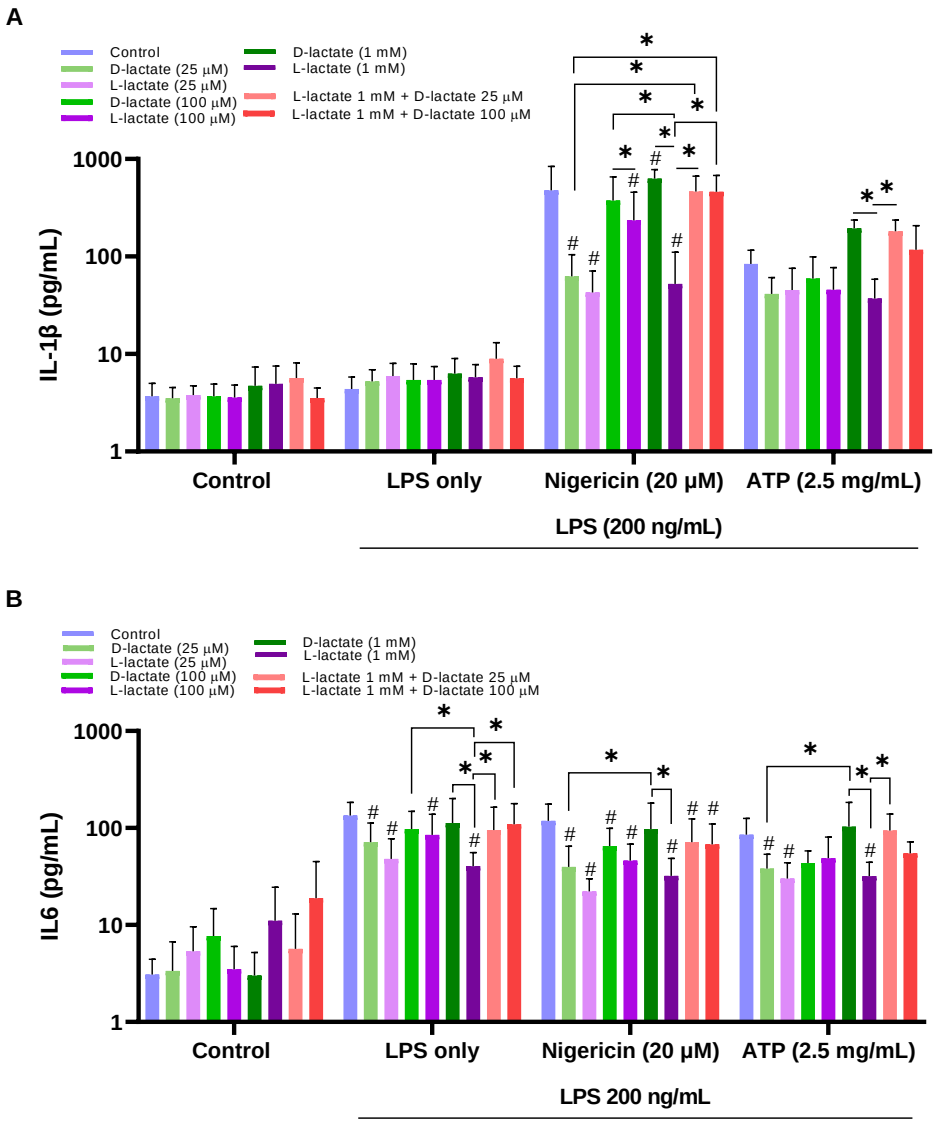

Figure 16: Cytokine production in response to lactate and NLRP3 inflammasome activators following endotoxin exposure in BMDMs.

IL-1β release (**A**) and IL-6 release (**B**) in BMDMs treated with D-lactate, L-lactate or D-lactate in the presence of L-lactate for 24 h and stimulated with nigericin (20 μM) for 30 min or ATP (2.5 ng/mL) for 1 h and LPS (200 ng/mL) for 4 h. Values are represented as mean ±SEM, n=6 for all groups where each replicate represents a separate day or animal. Significant differences between groups were found using Fisher's LSD test for normal data. *significantly different from the indicated group by two-way ANOVA. #significantly different from control by two-way ANOVA.

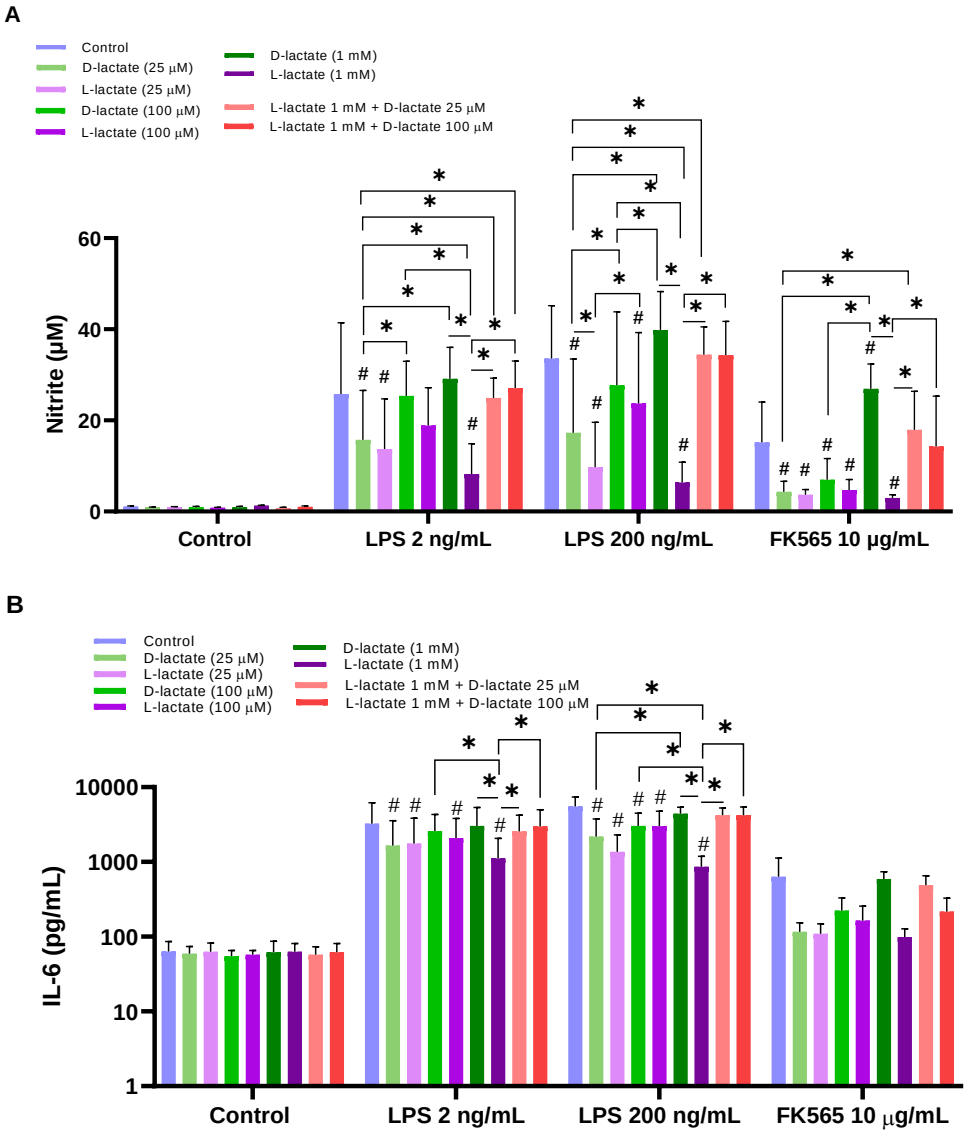

Figure 17: NO production in IFN-γ co-stimulated BMDMs during endotoxin or muropeptide exposure in response to lactate.

Measures of (**A**) nitrite release and (**B**) IL-6 release in BMDMs treated with D-lactate, L-lactate or D-lactate in the presence of L-lactate for 24 h and stimulated with LPS (2 ng/mL), LPS (200 ng/mL) or FK565 (10 μg/mL) and IFN-γ (10 ng/mL) for 16 h. Values are represented as mean ±SEM, n=9 for all groups where each replicate represents a separate day or animal. Significant differences between groups were found using a Fisher's LSD test for normal data. *significantly different from the indicated group by two-way ANOVA. #significantly different from control by two-way ANOVA.

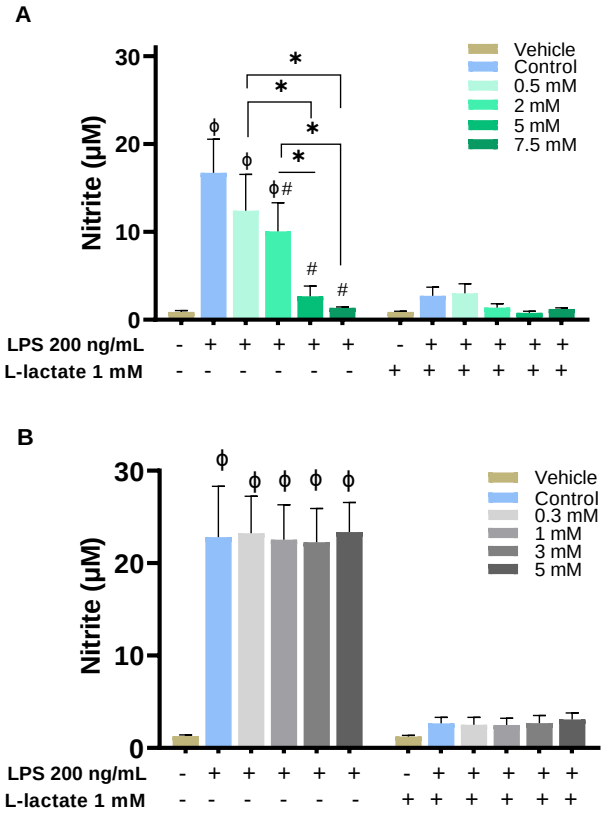

Figure 18: Effect of lactate transporter inhibition on nitrite release following endotoxin exposure in response to L-lactate in BMDMs.

Nitrite release in bone marrow-derived macrophages treated with L-lactate for 24 h and (**A**) αCHC (0.5 mM - 7.5 mM) or (**B**) 3-OBA (0.3 mM - 5mM) for 24 h and stimulated with LPS (200 ng/mL) for 16 h. Values are represented as mean ±SEM, n=6 for all groups where each replicate represents a separate day or animal. Significant differences between groups were found using Fisher's LSD test for normal data. *significantly different from the indicated group by two-way ANOVA. $^{\#}$significantly different from LPS by two-way ANOVA. $^{\phi}$significantly different from the vehicle by two-way ANOVA.